ISSN: 2642-1569

madridge PUBLISHERS
Interconnecting Scientific World

International
Journal of Earth Science and Geology

Research Article

Open Access

Paleoenvironmental Implications of Selected Siderite Zones in the Upper Atoka Formation, Arkoma Basin, Oklahoma-Arkansas: A Look Back and Current Views on Siderite Genesis in a Sedimentary Environment

Campbell MD[1]* and **M David Campbell**[2]

[1]*Senior Principal (Emeritus), Chief Geologist/Chief Hydrogeologist, I2M Consulting, LLC, Katy, Texas, USA*
[2]*Senior Principal and Program Manager, I2M Consulting, LLC, Katy, Texas, USA*

Article Info

***Corresponding author:**
Michael D Campbell
Senior Principal (Emeritus), Chief Geologist/ Chief Hydrogeologist
I2M Consulting, LLC
Katy, Texas
USA
E-mail: mdc@i2mconsulting.com

Received: September 18, 2018
Accepted: October 26, 2018
Published: November 19, 2018

Citation: Campbell MD, Campbell MD. Paleoenvironmental Implications of Selected Siderite Zones in the Upper Atoka Formation, Arkoma Basin, Oklahoma-Arkansas: A Look Back and Current Views on Siderite Genesis in a Sedimentary Environment. *Int J Earth Sci Geol.* 2018; 1(1): 6-40.
doi: 10.18689/ijeg-1000103

Published by Madridge Publishers

Abstract

According to the policy announced by the senior author (Campbell, 2017), this paper is based on data derived from the field work produced by the senior author during the mid-1970s as part of his research at Rice University. This paper covers field and follow-on sampling and evaluations developed from monitoring the literature on siderite genesis to date, including additional laboratory work on new samples obtained at the field sites, including incorporated carbonates and preliminary work on siderite remanent magnetism.

Occurrences in the two study areas of so-called 'clayband' and "black-band" siderite and zones of siderite-replaced marine fossils and associated sediments are reported in selected sandstone and shale sequences of the upper Atoka Formation of Arkansas and Oklahoma. Outcrops near Pocola, Oklahoma and Hackett, Arkansas were examined to characterize the paleoenvironmental conditions of deposition that may have promoted the genesis of siderite. Eight types of bedded or redistributed siderite were defined, each showing specific responses to bioturbation, to physical erosion and transport, and to chemical replacement and redistribution.

The clay minerals contained within the siderite zones and associated shale consist of kaolinite and illite in nearly equal proportions, with the former also possibly consisting of a kaolinite-type chamosite and the latter consisting of a significant 2M muscovite poly type. Interpretations based on sedimentary structures, texture and mineralogy of the sediments associated with the siderite zones indicate that specific sequences were likely deposited in a tidal flat or intra-deltaic environment in proximity to normal marine conditions. A primary or syngenetic origin is proposed for some of the bedded types of siderite occurrence. Other sequences indicate that marine conditions also prevailed. Physio-chemical requirements for siderite genesis suggest that siderite does not form syngenetically in a marine depositional environment but could syndiagenetically result under normal post-burial conditions involving organic-rich material (organic matter?) or a subsurface environment with a high Fe^{+2}:Ca^{+2} ratio and low SO_3 in solution. These conditions likely promoted characteristic siderization of calcareous material within marine sediments in proximity to or down the paleogeohydraulic gradient from areas of either syngenetically-produced siderite or iron-rich groundwater derived from coal-forming swamps.

Keywords: Siderite; Types of Siderite Occurrences; Pocola, Oklahoma; Hackett, Arkansas, Outcrops, Paleoenvironmental Conditions; Tidal Flat or Intra-Deltaic Environment; Stratigraphic Relationships; Mineralogical Characteristics; X-Ray Diffraction and X-Ray Photographic Studies; Fauna and Flora; Remanent Magnetism; Principal Carbonate Analyses; Thin-Section Analyses.

Introduction

Numerous thin ferruginous zones were reported in the upper Atoka Formation as early as the late nineteenth century [1]. Except for a casual interest in the ferruginous material as a potential iron ore, the zones have received little further attention with only occasional reports of "concretions" made during petroleum and coal exploration activities in the upper Atoka Formation over the past thirty years.

Objectives

The primary objective of this study was to evaluate the upper Atokan sediments and their character with a view toward defining the depositional environment of the sediments as related to the origin of the siderite. The study was designed to assess whether the siderite zones occurred in a preferred depositional environment, as indicated by sedimentary structures and other petrographic data, and to assess whether a unique mineralogical assemblage exists (or existed) within the sediments associated with the siderite zones that might have played a role in their origin. A definition of the character of the siderite zones is, therefore, required to determine whether the siderite is syngenetic, syndiagenetic or epigenetic in origin.

Subsidiary objectives of this study are to present field data and interpretations that may assist in defining the upper Atoka stratigraphy. The results of this study also have relevance to research on the development of the Arkoma Basin and its response to tectonism during Atokan time.

Location

Detailed examinations of two outcrops with reports of such ferruginous material were made, one outcrop just north of the town of Hackett in Sebastian County, Arkansas and the other just south of Pocola in Le Flore County, Oklahoma (See figure 1). The ferruginous zones, consisting predominantly of siderite, are associated with light gray, thinly bedded, fine-grained sandstone and dark gray to black shale.

Figure 1. Detailed examinations of two outcrops.

Procedure

Two outcrops were measured and described in detail. Samples were collected of: 1) the various siderite zones observed; 2) the associated sandstones and shales; and (3) the sandstones and shales that were not apparently associated with the siderite zones.

The local stratigraphic relationships in the Hackett and Pocola Sections are described in some detail to emphasize the depositional character of the sediments related to the siderite occurrences. Grain-size analyses and mineral identifications were made of selected samples within each of the sections measured, some associated and some not obviously associated with the siderite zones.

The morphological, mineralogical and biological characteristics of the ferruginous zones are described, followed by a review of siderite genesis in terms of its thermodynamic stability and in view of published descriptive and interpretative work on siderite.

A brief review of the general geologic setting involving stratigraphy and structure is given to serve as background to the ensuing discussion on the occurrence and genesis of the siderite zones. The following section describes the general stratigraphy of the Atoka Formation and other formations in the immediate area. The structural aspects are briefly treated in terms of the apparent impact of tectonic activity on sedimentation during the deposition of the Atoka Formation.

Geologic Setting

The regional geology is illustrated in figures 2 and 2a. The stratigraphy in the area is presented in figure 3. Haley [2] and Ballard [99] reported that parts of the Atoka Formation have distinctive lithologic characteristics. He defined two zones: Zone "P" near the middle of the formation and stratigraphically below the Hackett and Pocola Sections; and Zone ''W" in the upper third of the Atoka (approximately 2,600 feet from the top of the Atoka) and approximately 400 feet thick, composed predominantly of thin- to medium-bedded sandstone with minor siltstone and shale. The upper sandstone units of the Pocola Section are in Zone ''W" (See figure 2).

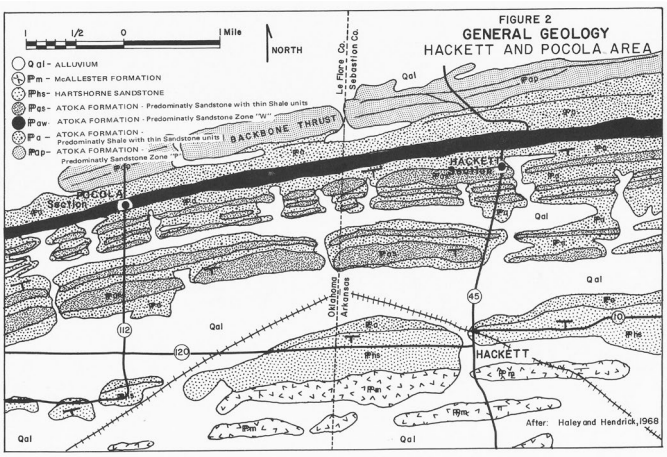

Figure 2. General Geologic Map Showing Sampled Sites: Hackett (Arkansas) and Pocola (Oklahoma).
Figure 2a. Detailed Geologic Map of Parts of the Greenwood Quadrangle.

The Hackett Section is stratigraphically above the Pocola Section. The uppermost sandstone of the Pocola Section is approximately 1,000 feet below the lowermost sandstone unit of the Hackett Section, likely separated by the predominantly black-shale sequence outcropping in the lower part of the Hackett Section and in the valley between the Hackett outcrop and the east-west trending Backbone Mountain to the north (See figures 2 and 2a). The sandstone units in the Hackett Section represent the first of five laterally continuous sand bodies above Zone ''W" of the Pocola Section.

Coal beds, although generally thin, have been reported in the Atoka Formation [3]. One of the coal beds (four inches in thickness) outcrops approximately 9.9 miles southeast of the Hackett Section near the top of Zone "W" and is known to extend eastward for approximately 45 miles. Another coal bed outcrops approximately 14 miles east-southeast of the Hackett Section near the top of the Atoka. The presence of an extensive coal bed within Zone ''W" suggests that at least part of the Pocola and Hackett Sections are either directly associated with non-marine units or are lateral equivalents. The coal will be discussed further later in this paper.

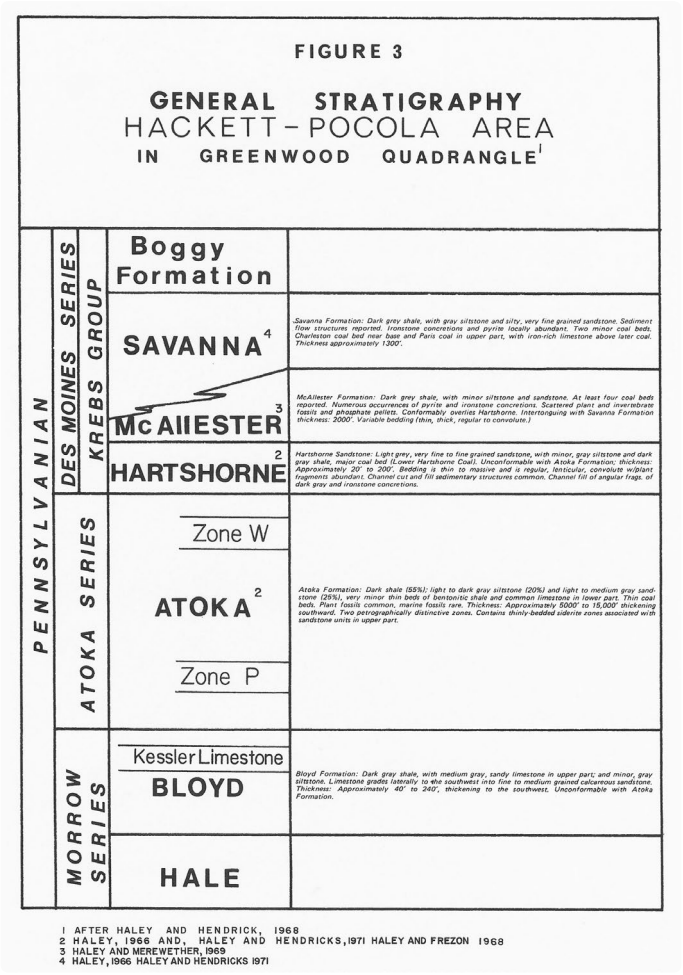

Figure 3. General Stratigraphy Hackeet-Pocola in Greenwood Quadrangle.

The Hartshorne Sandstone contains one major coal bed (the Lower Hartshorne Coal Bed), while the McAlester and Savanna Formations contain at least six thin and laterally discontinuous coal beds associated with shallow marine and non marine clastics [4].

General structure

The study area is approximately 25 miles north of the Choctaw Fault at the Arkansas-Oklahoma border (See figure 1), and is just south of the Backbone thrust (See figure 2). Haley and Hendricks [5] report that the subjects rock units have been folded into east-trending anticlines and synclines. At least two anticlines have been interrupted by listric thrust faulting and one syncline has been displaced by normal faulting. Haley and Hendricks [3] further suggest that the Atoka Formation is thinner where folded into anticlines and thicker where folded into synclines, and that where the Atoka changes thickness, all parts of the Atoka thicken or thin proportionately. They interpreted this characteristic as an indication that the anticlines and synclines were developing during deposition of the Atoka Formation, possibly influencing the pattern of deposition.

Buchanan and Johnson [6] have reviewed the structural history of the Arkoma Basin in the general area in terms of the regional tectonics and the effect on sedimentation. Table 1 is a summary of sequences, with the effects on the Hackett and Pocola areas indicated.

Table 1

TECTONICS AND SEDIMENTATION
HACKETT AND POCOLA AREA
(Modified after Buchanan & Johnson - 1968)

Time I	Basal Atokan Time: Deposition throughout flat shelf.
Time II	Lower Mid-Atokan Time: 1st normal faulting zone develops; contemporaneous deposition and subaerial erosion in places, involving Pocola-Hackett Sections; deposition south of area.
Time III	Middle Mid-Atokan Time: 2nd normal faulting zone develops south of Pocola-Hackett area with activity along 1st fault zone; erosion still affecting Pocola - Hackett area with deposition further south.
Time IV	Upper Mid-Atokan Time: 3rd normal faulting further south; erosion still affecting Pocola and Hackett area with deposition further south.
Time V	Upper Atokan Time: Cessation of normal faulting; deposition of Upper Atokan in Pocola and Hackett area (Zone "W" marker).
Time VI	Desmoinesian: Clastic deposition over wide area; no major tectonic activity; major and minor coal beds.
Time VII	Post-Desmoinesian: Development of northward directed, laterally-compressive orogenic forces; severe deformation and listric thrusting of Atokan sediments south of Choctaw fault zone, grading northward to less severe thrusting and folding, e.g. east-west elongate anticlines and synclines and Backbone thrust.

Table 1. Tectonics and Sedimentation. Hacket and Pocola Area.

Briggs and Roeder [7] reviewed plate tectonic models applicable to the development of the Arkoma Basin. A regional understanding is developing via Suthernland [8], who has summarized the work through 1988 in an interpretation illustrated in Figure 3a. This is based on the work by Kolnm and Dickey [9]; Vedros and Visher [10]; Houseknecht and Kacena [11]; Zachry [12]; Grayson [13]; Sutherland [14]; Zachry and Sutherland [15]; and Houseknecht [16]. The basin has received increasing attention from the oil and gas industry over the years.

Suneson [17] provided an excellent summary on the history of the basin and defined formally named stratigraphic units – those identified and described from surface outcrops

and called out in the professional literature, from informal units used by those typically identified in the subsurface and applied by industry geologists.

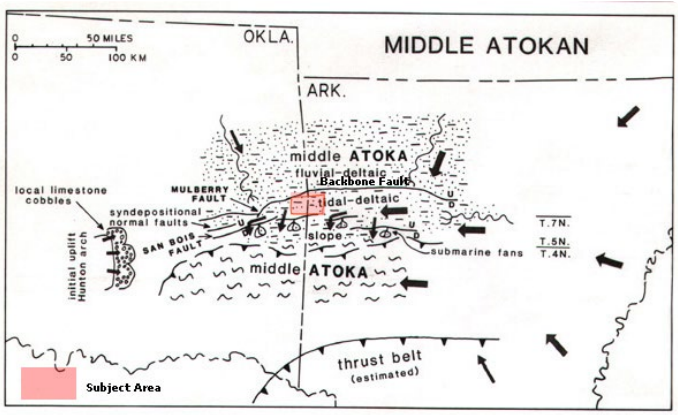

Figure 3a. Upper to Middle Atokan Paleogeographic Map [68].

Hackett and Pocola Sections

The local stratigraphy of both the Hackett and Pocola Sections is treated in some detail to emphasize that, although the Hackett Section is stratigraphically above the Pocola Section, the scattered zones now consisting of siderite that occur in both sections occupied a similar depositional environment. As will be shown, erosion and redeposition of previously deposited sediment is the dominant depositional process. Fluctuations in bottom current velocity and direction, expressed by various sedimentary structures and fluctuations in sedimentation rate expressed by variations in bed thickness, combined with a non-indigenous marine fauna in thin fossil debris zones, are features characteristic of a prograding shallow water deltaic tidal flat environment. The uniformity of sediment texture and mineralogy of the sandstone beds suggest multiple periods of erosion and redeposition.

As will be proposed, the zones now consisting of siderite were either organic material (fecal pellets?) or iron-rich (Fe^{+2} and Fe^{+3}) sediment concentrated by bottom currents during periods of slow deposition. The material became a gel-like mud and was either syngenetically altered to siderite or syndiagenetically altered first to chamosite (and/or pyrite) during the early stage of burial and microbial activity (sulphate reduction). Subsequent to the completion of sulphide reduction and with the introduction of additional Fe^{+2} from interstitial solutions, syndiagenetic siderite was formed.

One critical problem regarding the genesis of siderite is whether the zones now occupied by siderite were in fact previously occupied by organic material syndiagenetically altering to siderite with an intermediate precursor of chamosite and/or pyrite, or were primary sites of iron carbonate accumulation. Evidence to support either process is indirect, but present physio-chemical theory seems to preclude a primary or syngenetic process of direct precipitation of siderite at the depositional surface under marine conditions. If the siderite can be shown to be a primary chemical precipitate, then a lagoonal or tidal flat depositional environment can be inferred for at least some of the intervals of the Hackett and Pocola Sections. Other sequences can be interpreted as indicating a paralic or intradeltaic depositional environment. It is toward the solution of this problem in interpreting depositional environment that the following lithological, textural and mineralogical descriptions are directed.

Stratigraphy-Hackett section

The measured section for the Hackett outcrop is illustrated in figure 4. The section consists of approximately 160 feet of sediment with dark gray shale in the lower interval grading to a dark to light gray shale-siltstone and to sandstone units in the upper part of the section.

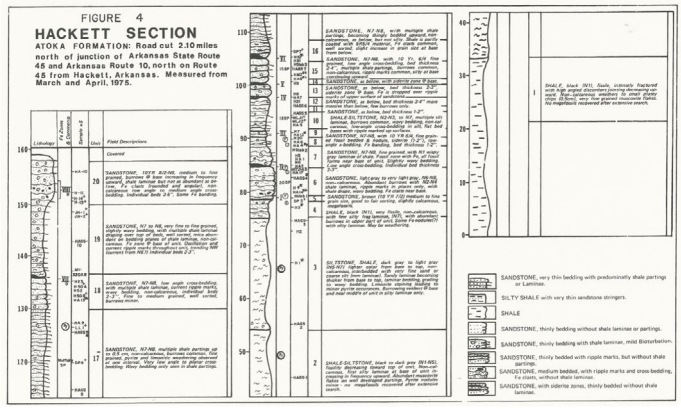

Figure 4. Hackett Section Atoka Formatation: Road cut 2.10 miles north of junction of Arkansas State Route 45 and Arkansas Route 10, north on Route 45 from Hackett, Arkansas. Measured from March and April, 1975.

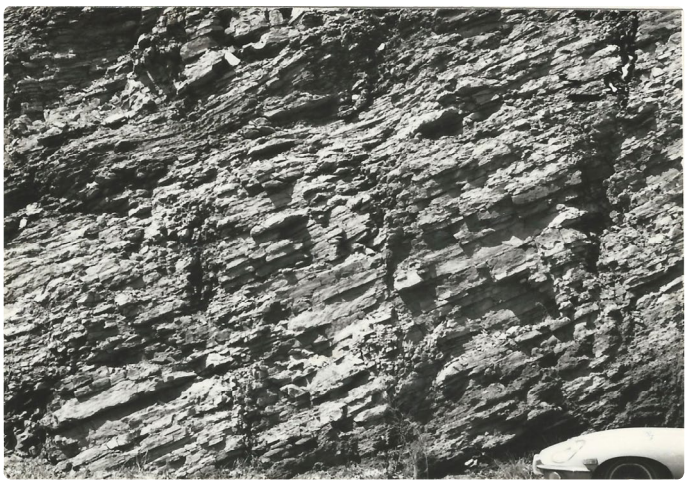

Figure 5. Hackett Section: Outcrop View showing Units 4, 5, and 6. See figure 4 for Location of Units. Siderite Zones Type I and II. Unit 4 Shale Upper Contact at Nose of Jaguar.

The west wall of the Hackett outcrop is illustrated in figure 5. Unit 4 (as defined in figure 4) is shown at the nose of the XKE Jaguar. No fossils were recovered in the shale units, but burrowing was noted at the base and in the middle of Unit 3. An increase in the number of light gray silty laminae were noted, with the first silty laminae at the base of Unit 2, increasing in number and thickness up through Unit 3 to a maximum thickness of a few millimeters. Bedding changes from flat in the predominantly shale section to wavy in the silty laminae zones of Units 2 and 3. Small pyrite nodules were noted in both units. All shales are non calcareous.

Unit 3 grades into black, very fissile shale (Unit 4), that has abundant burrows in the upper part and a sharp upper contact. Unit 4 is overlain by a thin light brown (10YR7/2), calcareous sandstone containing abundant burrows, gastropods, pelecypods, and echinoid and crinoid plates and spines (Faunal content is treated later). The contact between Unit 4 and the thin light brown sandstone containing ferruginous "fossil hash" and thin massive siderite zones of Unit 5 (Fe Zone I) are shown in figure 6. All ferruginous material, as will be described in detail later, is predominantly siderite, with minor and various other minerals.

Beginning with Unit 5, and continuing to the top of the section, abundant thinly-bedded, partly tabular sandstone with shale laminae occur. The light gray sandstone beds vary in thickness from 2" to 5" with occasional beds of up to 8". Thin shale laminae or partings are draped over the top of many beds on a ripple-marked surface. Some ripple-marked beds have a thin film of black (and some red) shale (e.g. Unit 16).

Figure 6. Hackett Section: Close-Up Outcrop View of Unit 4-Unit 5 Contact Type III Siderite Zone I. Note Burrowing in Lower Shale Unit and Dark Banding at Mid-Point of Hammer Handle, Tabular Bedding.

Low angle cross-bedding, wavy bedding, bioturbation and trace fossils (in certain intervals, e.g. See figure 4) are characteristic for the intervals from Unit 6 through Unit 16. Siderite zones occur at various intervals within this group, as will be discussed in detail later. Shale partings are discontinuous as are the individual sandstone beds. Shale laminae pinch-out in the sandstone beds along ripple-marked surfaces. The sandstones that show low angle cross-bedding are truncated at various angles by the uppermost ripple-marked surface (flaser bedding). Ferruginous clasts (sideritic) are common at the base of Unit 6, within Unit 16 and in the lower part of Unit 20 near the top of the section. Fossil debris zones (sideritic) also occur in Units 7 and 9 (and Unit 5).

The base of Unit 7 and a ferruginous fossil debris zone just below hammer are shown in figure 7. Unit 17 marks a change in lithology where multiple shale partings become more abundant than in the units below. The partings are wavy to planar laminae (up to 1") interbedded with fine-grained sandstone. Nodular pyrite was recovered near the top of the unit. Tops of some beds are ripple-marked, others are planar. Beds are also lenticular but shale partings appear more continuous than those lower in the section. Top of the unit appears to be conformable with Unit 18.

Figure 7. Hackett Section: Outcrop View of Type III Siderite Zone II. Note Fossil Debris Zone (Dark Banding) at Right.

Unit 18 shows a decrease in shale laminae and an increase in ripple-marked surfaces (current ripple-marked surface are common in unit). Burrows and trace fossils are minor. Unit 19 is characterized by the abundant mica flakes on the bedding surfaces of the black-shale laminae and by the oscillation and current ripple-marked surfaces trending northwest near the middle of the unit.

Siderite zone VII (as defined in figure 4) is shown in figure 8 near the bottom and associated bioturbated sandstone and shale laminae at the top. The uppermost Unit 20 shows an increase in grain size, a decrease in shale laminae and abundant siderite clasts near the base of the unit. Ferruginous banding within individual beds is conspicuous, a type of siderite occurrence discussed later.

Figure 8. Hackett Section: Close-Up Outcrop View of Type I Siderite Zone VII. Note Siderite Zone Near bottom of Photograph. Pipe Bowl is 5 cm High Stratigraphy-Pocola Section.

Stratigraphy - Pocola Section

The measured section for the Pocola outcrop is illustrated in Figure 9. The Pocola Section is stratigraphically lower than the Hackett Section; based on dip and lateral separation of the two sections, the uppermost sandstone of the Pocola

Section is approximately 1000 feet below the lowermost sandstone unit of the Hackett section, probably separated by the predominantly black shale sequence outcropping in the valley between the Hackett outcrop and the east-west trending Backbone Mountain to the north.

Briggs et al. [18] indicate that this section is approximately 2,600 feet stratigraphically below the top of the Atoka Formation. Thrust-faulted contacts are mapped in the lower part of the Pocola outcrop (See figure 2), but were not apparent in the field. The sandstones of the Pocola Section are within Zone ''W", as after Haley [2].

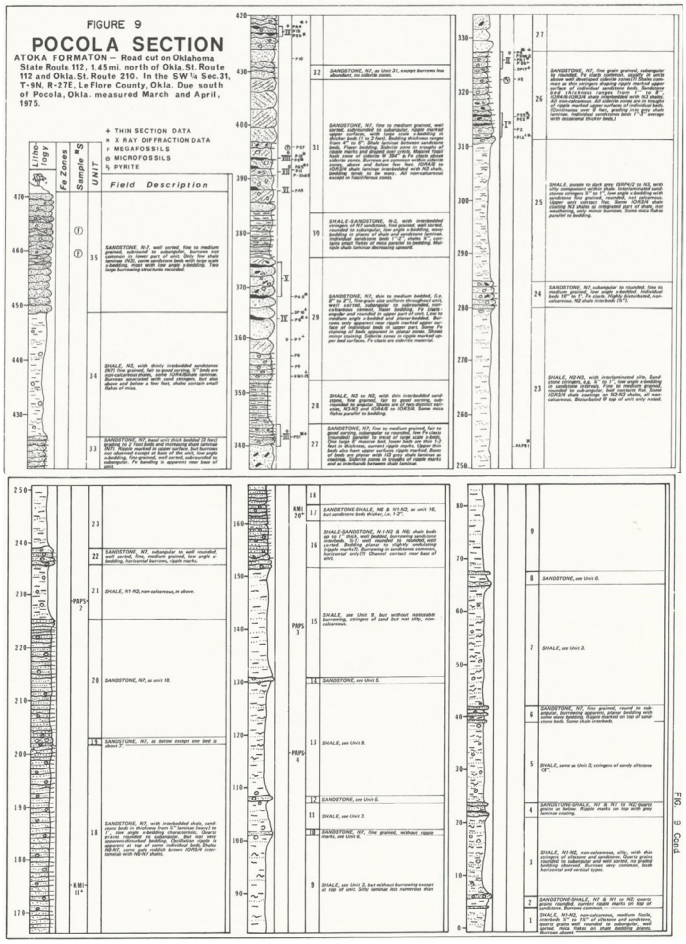

Figure 9. Pocola Section Atoka Formation-Road cut on Oklahoma State Route 112, 1.45 mi. north of Okla. St. Route 112 and Okla. St. Route 210. In the SW$^{1/4}$ Sec. 31, T-(N, R-27E, Le Flore Country, Okla. Due south of Pocola, Okla. Measured March and April, 1975.

The Pocola outcrop consists of approximately 470 feet of vertical section, as indicated in figure 9, the lower 150 feet of section is essentially dark silty shale units with lighter thinly laminated siltstone. The 150 foot interval is regularly punctuated by thin sandstone beds up to 3 inches in thickness. Up to three such beds make up the sandstone units, separated by dark silty shale of the predominantly shale units.

The lower sandstone units (Units 2, 4, 6, 8, 10, 12, and 14) are light gray (N-7), uniformly fine grained, well sorted, angular to rounded, with occasional ripple-marked upper surfaces and sharp contacts at the base of sandstone overlying shale. Bioturbation is common but not abundant (horizontal and vertical burrows). Obvious grading within the sandstone units was not observed. Bedding is commonly laminar but some wavy bedding was recorded. Sideritic zones were not observed.

The dark silty shale units (Units 1, 3, 5, 7, 9, 11, 13, and 15) are non calcareous, with medium fissility, micaceous and occasional horizontal and vertical burrowing structures. Siltstone and fine sandstone stringers are 1/4" to l1/2" in thickness with regularity in the units. Unit 15 shows a gradational increase in sand-size material in the thin stringers. Burrowing is conspicuously absent.

A major change in sediment character occurs in Unit 16, approximately 150' above the base of the measured section. The unit has a sharp contact at the base. The predominantly shale unit below, increases in sand-size material, producing numerous sandstones 1/2" to l" in thickness in Unit 16, with shaly intervals up to 1" thick. Burrowing is common in the sandstone, near horizontal structures only (?). A significant feature of the lower part of Unit 16 is the presence of cut-and-fill surfaces in the thicker sandstone beds (>1 foot thickness). Sideritic material was not recorded. Unit 16 shows a gradational increase in sand content and decrease in shale. Both top and bottoms of the individual sandstone beds are flat.

Unit 18 is significant because of the first appearance of well-developed, low-angle cross-bedding. Bedding is disturbed in places as a result of heavy bioturbation. Current ripple marks are apparent on the upper surface of some beds. Measurement of the dominant forms, where possible, indicates a 4 inch wavelength, trending north to northwest. Some Ripple marks, however, are complex oscillation forms; some are faintly polyhedral (?).

Units 18 through 20 (a 60 foot interval) are predominantly sandstone units. Unit 19 is thicker than the beds below and above, approaching 2 feet. Sandstone bed thickness in Units 18 and 20 is variable (thin mm laminae to 12" beds). Burrowing is abundant in places and contains oscillation ripple marks. A particular characteristic is the pale reddish-brown shale (10R5/4) interlaminated with N6-NS shale.

Unit 25, a twenty-five foot interval, is distinctive by its sideritic component (5RP4/2) within the dark shale which is common below. The dark purple laminae are separate in places and merge into N-3 shale laminae along the bedding plane.

Unit 26 is predominantly a sandstone unit with individual beds ranging in thickness from 1 inch to 8 inches and contains the first two sideritic zones (Zones I and II-See figure 9 for location in section). Thin shale laminae are common and drape the upper ripple-marked surface of individual sandstone beds. Shale (of the color: 10R4/6 to 10R3/4) are interlaminated with N-3 shale laminae. Sandstone grain size and angularity are very similar to all units below (i.e. fine grained, sub angular to sub rounded). The unit contains abundant burrowing features, e.g. horizontal and vertical burrows, disrupted bedding, and numerous trails on bedding planes, especially on the bottom of individual sandstone beds coated with laminae of N-2 shale. Sideritic clasts are common above Zone I and in Zone II, where abundant echinoid fragments were recorded, replaced by sideritic material. Pyrite is recorded near the middle of the unit.

Unit 27 is a distinctive unit of massive, relatively thickly bedded sandstone with medium to large scale cross-beds. One six-foot bed also contains sideritic clasts oriented parallel to the cross-set trends. Other beds are 1 to 2 feet in thickness, some containing ripple-marked upper surfaces, sideritic clasts, and burrows. Flaser bedding is ubiquitous. Zone III is in the upper part of Unit 27, containing sideritic bands 1 to 2 cm in thickness and abundant echinoid fragments.

Unit 27 grades into Unit 28, becoming more shaly than the shale in Unit 27. Bedding is flat with thin laminae of fine grained, sub rounded to angular sandstone. Two distinct and separate laminae are present, e.g. the N3-N2 dark gray shale and 10R4/6 to 10R3/4 shale. Mica is locally abundant on irregular shale bedding surfaces (ripple marks?). Figure 10 shows the character of the massive bed grading into Unit 28.

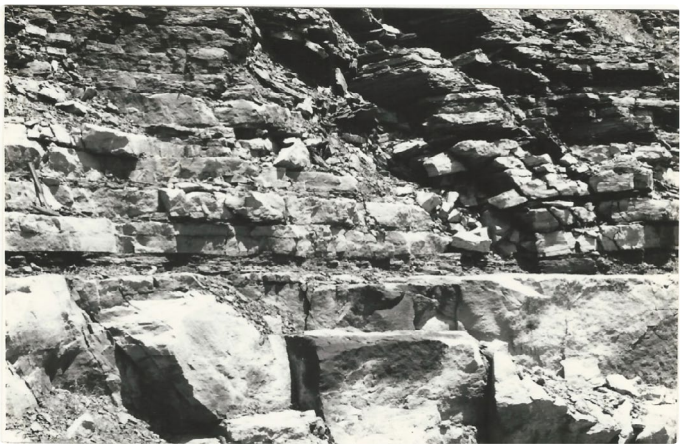

Figure 10. Pocola Section: Outcrop View of Massive Sandstone (Unit 27 in Figure 9) and Thinly Bedded, Shaley Sandstone (Unit 28) Transition. Note Hammer for Scale Left Center of Photograph.

Unit 28 abruptly changes to a dominantly sandstone Unit 29, distinctive for the absence of multiple shale partings. Near the base of the unit, fairly thin beds (e.g. 2-6") are marked by very thin shale laminae, decreasing to films on the more massive thickly bedded and ripple-marked sandstone higher in the unit. Low to medium angle cross-beds is apparent in the thicker sands. The thinner beds are bioturbated; the thicker beds are without noticeable burrowing. Echinoid plates are recorded in a sample of the massive unit. Siderite Zones IV and V occur at the top of two of the massive beds. Figure 11 shows Zone IV and V, with the ferruginous banded zone clearly evident just above a massive sandstone bed.

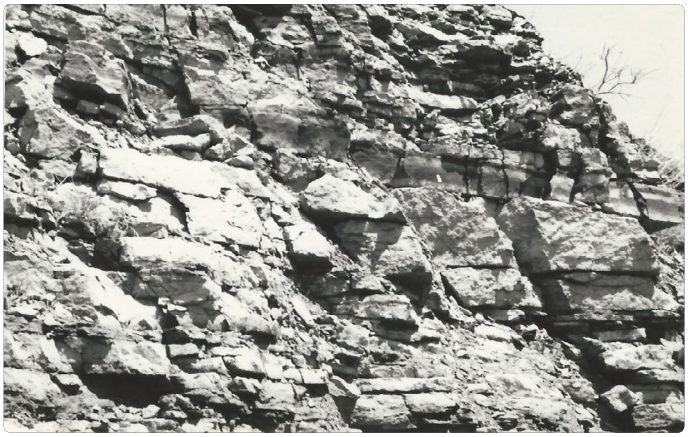

Figure 11. Pocola Section: Outcrop View of Type IV-A Siderite Zone IX. Note "Massive" Beds and Ferruginous Banding.

The ferruginous banding, a few burrows, clasts and part of Zone V just above are shown in figure 12 below.

Figure 12. Pocola Section: Close-Up Outcrop View of Ferruginous Banding: Type IV-A Siderite Zone IX Shown in Top Right of Figure 11.

A highly bioturbated bed just below a ferruginous banded zone above is shown in figure 13. Unit 30 is a shale-sandstone sequence with multiple shale laminae at the bottom decreasing in number upward (for location in section, see figure 9).

Figure 13. Pocola Section: Close-Up Outcrop View of a Type IV-A Siderite V. Note Bioturbated Sandstone Overlain by "Massive" Sandstone Unit with Ferruginous Banding.

The upper-most coherent siderite occurrence within the measured section is shown in figure 14 representing the transition between Unit 29 to Unit 30. Note siderite near bottom overlain by massive sand with scattered siderite clasts, which is overlain by a planar bedded interval grading to the wavy-bedded, multiple shale laminae of Unit 30.

Unit 31 is a sequence of relatively massive sandstone with only very minor shale laminae as films on the upper ripple-marked surface of individual beds. High- to medium-angle cross-bedding is evident in some beds. Three discontinuous siderite zones (VI, VII, and VIII) occur at the base of some beds. Burrows are common in beds containing the siderite zones and above and below. Sandstones are fine to medium grained, well sorted and subrounded to subangular. Of special significance is Zone VIII where a massive 'fossil hash" zone was recorded, which is discussed later.

A shale (10R4/6 to 10R3/4) is interlaminated with wavy bedded N-3 shale. Siderite was not reported in the upper part of Unit 31, although beds appear identical in character to those of Unit 31 containing the siderite zones.

Figure 14. Pocola Section: Close-Up Outcrop View of Unit 29 – Unit 30 Transition. Note Gradational Sequence from Bottom to Top. Type I Siderite Zone Showing at Bottom Right. Also "Massive" Sandstone with Siderite Clasts (e. g. of Type IV), Just above Showing Planar Bedding, and Wavy Bedding of Shale Laminae near Top of Photograph.

Stratigraphic comparisons: Hackett and Pocola sections

In general, a number of differences exist between the Pocola and Hackett Sections:

1. Massive sandstone beds with medium to high angle cross-bedding are more numerous in the Pocola than in the Hackett Section;
2. Siderite clasts associated with massive sandstone beds are more numerous at Pocola than at Hackett;
3. Siderite banding unassociated with macro-fossil debris zones are present at Pocola and not present at Hackett;
4. Macro-fossiliferous siderite zones are less numerous at Pocola than at Hackett;
5. Bioturbation is apparently less common at Pocola than at Hackett;
6. Shale laminae are less numerous at Pocola than at Hackett; and
7. Relatively large scale cut-and-fill structures were recorded at Pocola, not at Hackett.

Strong similarities still, however, exist between Pocola and Hackett Sections:

1. Bedding types (laminar, planar, wavy and flaser).
2. Presence of ripple-marked upper surfaces draped by thin films of shale.
3. Thinly bedded sandstone units and other lithologic and biologic features, including the occurrences of siderite, to be discussed in detail later in this paper.
4. Thin, massive siderite occurs in the ripple-marked upper surfaces of some sandstone beds.
5. Thin siderite bands occur as discrete laminae within the thin black shale laminae, and
6. Common heavily bioturbated intervals.

The notable paeloecological features exhibited in the Hackett and Pocola Sections are:

1. thinly bedded sandstone and associated shale laminae show current and oscillation ripple marks, wavy, laminar and flaser bedding, indicating gentle to mild fluctuating currents;
2. thinly bedded sandstone with erosional surfaces (ripple marks and low angle cross-bedding) draped in some locations by thin films of black shaly material show strong regularity, suggesting periods of rapid deposition followed by periods of very slow deposition. This also may indicate numerous periods of erosion of previously deposited sediment;
3. thickly bedded sandstone show massive, planar, low to medium angle cross-bedding with occasional siderite clasts indicating fluctuating multidirectional bottom current velocities from gentle to fairly strong currents, the latter associated with distributary channels;
4. bioturbation is apparently less common at Pocola than at Hackett and probably related to the volume sediment available to constitute the massive sandstone units at Pocola;
5. All features above indicate a tidal-flat or intra-deltaic environment, within proximity to a marine environment [19,20]; (See "Environment of Deposition" herein for additional discussion).

Textural character-Hackett section

In order to characterize the textural aspects of the sediments in the section, samples were selected at intervals. The samples are either associated or unassociated with the siderite zones. Grain-size analyses were made of twelve samples, with three replicate analyses for calculation of standard deviation (See Appendix A for procedure adopted).

Two hundred counts per thin-section were made incorporating the longest diameter encountered during the thin-section traverses. A total counting error for Mz, including analytical plus sampling errors was calculated to be approximately nine percent. Total error for σ_i=11% and for Sk_i=34%. Since the sampling errors are excessive for the latter two textural features, the parameters were not used for interpretation. Mz errors are, however, within acceptable limits (The cumulative arithmetic curves for the samples counted, and also for the associated ferruginous zone and unit samples, are included in Appendix A).

Sampling objectives for the study of the textural characteristics of the lithologic units examined were: 1) define apparent transition zones, 2) characterize "typical" samples from certain intervals of interest; and 3) examine the vertical variations in Mz values to the extent the data permit. Figure 15 is a summary and vertical comparison of the data over a 75-foot interval (Units 5 through 20). The Graphic Mean (Mz) is shown with respect to the vertical location of the ferruginous zones and types to be defined later. Error bars for three samples are also shown [21].

In considering the graphic mean grain size, figure 15 shows a fining sequence upward in the lower sandstone units,

followed by an interval of constant grain size, which in turn is followed by a second fining upward sequence. Near the top of Unit 17, a coarsening upward sequence begins and extends over less than 10 feet, followed by a third fining-upward trend, terminating by the onset of a second coarsening upward sequence.

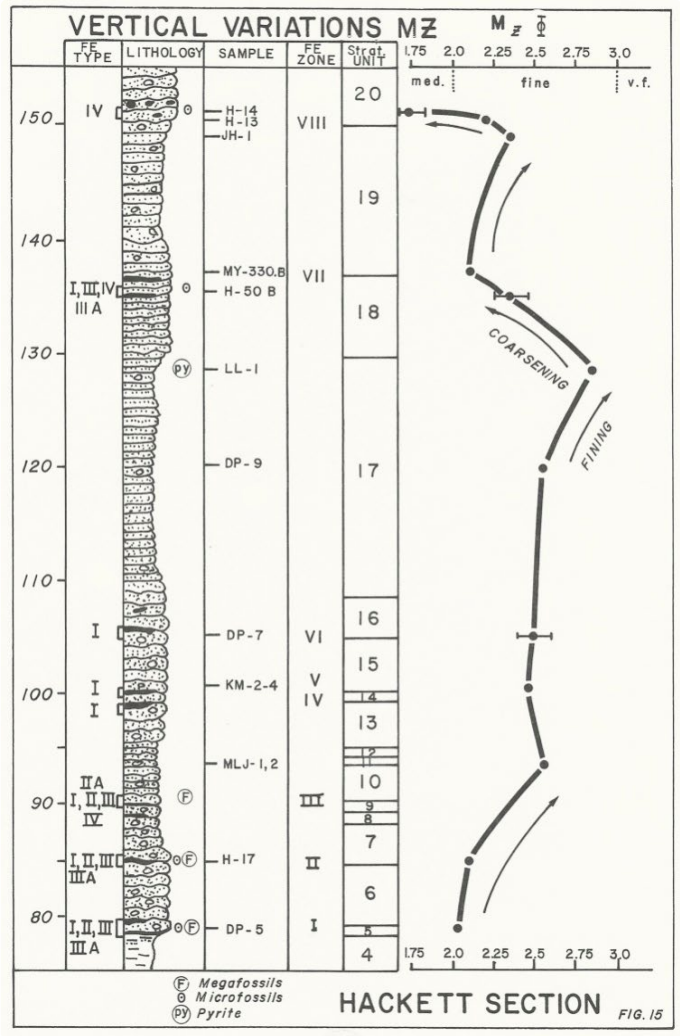

Figure 15. Vertical Variations Hackett Section

Textural character-Pocola section

A grain-size analysis was also made of twelve samples with three replicate analyses for calculation of standard deviation of total counting errors. Cumulative-arithmetic curves were prepared (See Appendix A). A vertical grain size (Mz) comparison over a 110 foot vertical interval of the Pocola Section is illustrated in figure 16 with Units. 17, 18, and 26 to 33). Error bars for three samples are also shown.

It became clear during the field work that the units at the Pocola Section were significantly different from those at the Hackett Section. The basis for setting unit boundaries during this study was defined. The Hackett Section contains many thin, but definable, units, whereas at Pocola the units are generally thicker reflecting the presence of more massive beds. Twelve samples were taken over a 75 foot interval at the Hackett Section. One sample, therefore, grossly reflects 6.3 feet of section. At Pocola, since the units were thicker, twelve samples were taken over a 110 foot interval, where one sample represents about 8.9 feet of section. Therefore, if Mz trends were reasonably apparent at Hackett, then trends should have been apparent at Pocola, if processes were similar. A vertical spread was therefore achieved.

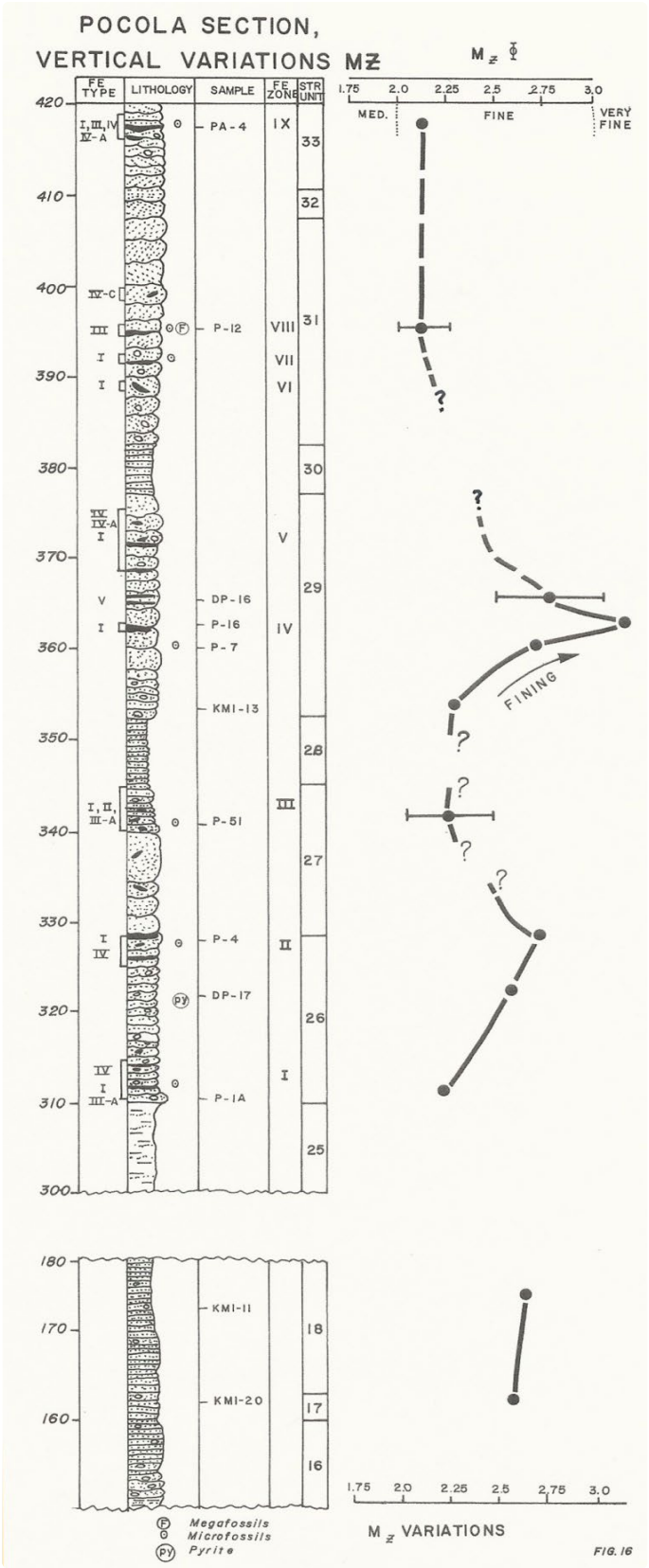

Figure 16. Pocola Section, vertical Variations

Specific sampling sites of "typical" samples from important units were made where obvious in the field. However, it is felt that although "typical" samples were obtained, samples from

some important units were not obtained, e.g. lower Unit 27, Units 28 and 30, because the Units 28 and 30 are predominantly shale units with abundant, poorly bedded, very thin sandstone beds. Transition samples were taken in Unit 29 at unusually closely spaced intervals by using the obvious change in lithology as a guide in the field. Other similar transitions were not obvious in outcrop and sampling objective (3) was exercised to obtain spread. It is clear, therefore, that although the beds are more massive at Pocola than at Hackett, they may not be as uniform in character as suggested in the field.

Unit 26, the first unit containing siderite zones, shows a decrease in Mz from base to top of unit. Siderite Zone I is at the base of the unit and Zone II is recorded at the top of the unit with clasts associated with both zones. A sampling break occurs within Unit 27. Zone III sandstones contain clasts and a point-source Mz similar to Zone I.

Unit 29 shows a good fining-upward trend. Lithologically, the beds at the base of the unit are thinly bedded and become massive up the unit, suggesting an increasing sedimentation rate, a decreasing current velocity and/or a mixing of sediment source and reworking of previously deposited sediment locally. Shale laminae are not common, but siderite Zone IV occurs within the fining sequence at the upper surface of one of the massive sandstone beds.

Medium scale (and small-scale cross-bedding and planar bedding) were reported, the latter in an interval containing ferruginous banding just above the transition from a fining-upward sequence to a coarsening-upward sequence, a sample break making a clear trend tentative. The features indicated in the interval suggest that a high-energy condition was dominant in the sequence. Units 31 through 33 appear to be uniform in Mz. This interval is characterized by massive bedding, with some thinly bedded sandstone with very minimum shale laminae and high-angle cross-bedding, incorporating siderite Zones VI, VII, VIII and IX of clasts, massive and "fossil hash" sideritic material, to be discussed later. Individual sandstone beds are also characterized by flaser bedding within the beds on a large scale and on the upper surfaces, suggesting a relatively high energy multidirectional process and a relatively high rate of deposition.

Units 17 & 18, considerably below the first occurrence of siderite zones are shown in figure 17. The data available show that the dominant processes and depositional conditions may not have been different from those of the intervals containing siderite zones, which suggests that the materials used to form the siderite arrived in part after deposition of the sediments, but also just after soft sediment reworking to incorporate clasts of siderite.

Textural comparisons: Hackett-Pocola sections

Although considerable similarities exist between the Pocola and Hackett Sections, the differences overshadow the similarities. It is apparent that Mz combined with sedimentary structures indicate fluctuating energies of transport, punctuated by periods of erosion and reworking. The numbers of beds containing clasts, as mentioned, are greater at Pocola than at Hackett, suggesting that the massive beds represent periods of relatively high energy currents. Although the beds are generally more massive at Pocola, a comparison of grain size suggests that the sedimentation rate could have been higher at Pocola than at Hackett. Table 2 is a summary comparison of Mz, σ_I, and Sk_I for Pocola and Hackett Sections. The use of σ_I and Sk_I, however is of doubtful value on the basis that sampling errors involved in counting produce high standard deviations at the 95 percent level.

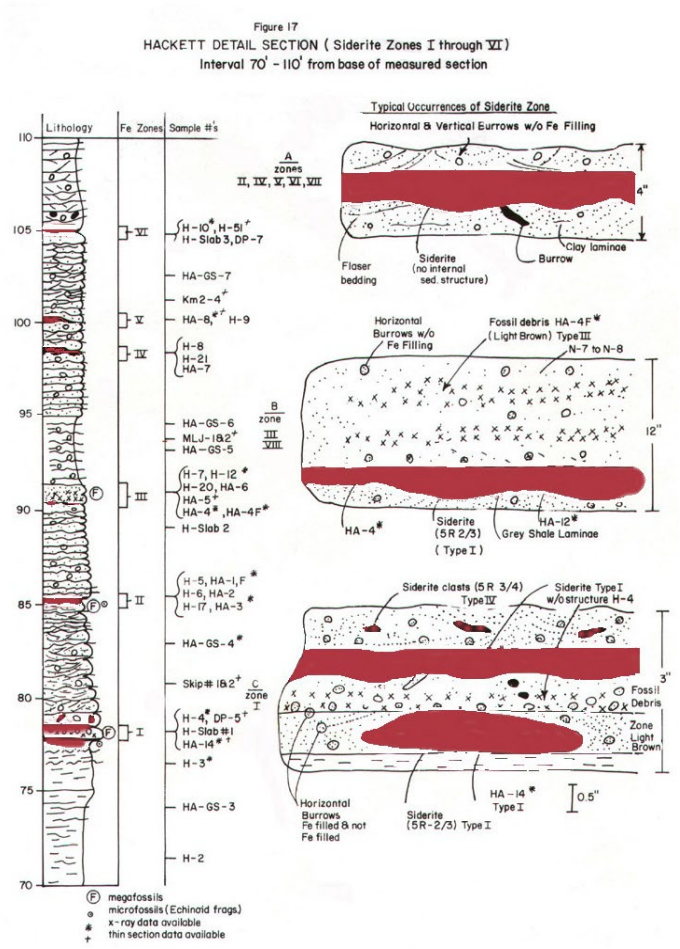

Figure 17. Hackett Detail Section (Siderite Zones I through VI). Interval 70'-100' from base of measured section

Table 2

M_Z, σ_I, Sk_I AND STANDARD DEVIATION
POCOLA AND HACKETT SECTIONS

	Pocola	Hackett
Grain Size		
M_Z - Range	2.10ϕ to 3.19ϕ	1.72ϕ to 2.80ϕ
Ave.	2.54ϕ ± 8.6%	2.33ϕ ± 8.6%
Sorting		
σ_I - Range	0.33ϕ to 0.59ϕ	0.38ϕ to 0.60ϕ
Ave.	0.43ϕ ± 11.2%	0.45ϕ ± 11.2%
Skewness		
Sk_I - Range	-0.15 to +0.33	-0.09 to +0.35
Ave.	+0.13 ± 33.8%	+0.17 ± 33.8%

Table 2. M_z, σ_I, Sk_I and Standard Deviation Pocola and Hackett Sections

Mineralogical character-Hackett section

Mineral identification and abundance were first estimated for the twelve thin-sections used in the grain size analyses of figure15 and then by X-ray diffraction for confirmation, when possible. The results of the visual estimation are given in table

3. All percentages shown exclude ferruginous material and were obtained by the multiple field of view averaging technique. The relationship of the particular sample with the designated siderite zones and type of occurrence (to be discussed later) are shown.

Table 3

HACKETT MINERAL IDENTIFICATION AND ABUNDANCE ESTIMATION

Fe Zone	Type	Sample#	Heavy Min.	Percent(1) Qtz & Chert	Calcite	Clay Min.	Micas	Plag.	RF
VIII	III	H-14	< 1	85	5	5	3	1	1
VIII	III	H-13	< 1	85	5	5	3	1	1
*		JH-1	< 1	85	3	7	1	3	1
*		MY330-B	~ 1	85	nil	12	< 1	2	1
VII	I	H-50B	< 1	85	2	10	< 1	2	1
*		LL-1	< 1	85	nil	10	3	2	< 1
*		DP-9	< 1	80	1	15	3	2	< 1
VI	I	DP-7	< 1	75	2	20	1	1	1
*		KM2-4	< 1	75	2	20	1	1	1
*		MLJ-2	< 1	75	2	20	1	1	1
II	I	H-17	< 1	80	8	10	1	1	1
I	III	DP-5	< 1	70	10	14	4	1	< 1
		Ave.	< 1	80	3.3	12.3	1.8	1.5	< 1

(1) All counts excluded Fe material (multiple field of view averaging)
* Indicates interval from which sample was taken is not associated with a siderite zone

Table 3. Hackett Mineral Identification and Abundance Estimation

Quartz, of course, constitutes the largest mineral component of the sediments examined, with calcite, mica-clay minerals, plagioclase, and heavy minerals (zircon and tourmaline), in addition to siderite-replaced calcite and massive and laminated siderite. The sandstone units are essentially quartz arenites.

Quartz occurs as discrete detrital particles and is subrounded to subangular with elongate and subsequent shapes. Some grains show strong strain shadows and some show overgrowths. Crenulated boundaries and the minor occurrence of composite grains suggest a metamorphic origin for that quartz. Detrital chert is uniformly present in most of the samples unassociated with siderite zones and is probably easily degraded over numerous periods of reworking so a relatively near source is suggested. The presence of calcite is related to the occurrence of fossiliferous material occurring as discrete fragments (partly to wholly replaced with siderite) and as scattered heavily altered cement. Pyrite is recorded within burrow structures and as small masses within thinly bedded sandstone with quartz overgrowths.

A brief description of each of the thin-sections used in the above characterizations is given in Appendix B. Emphasis is placed on: 1) quartz angularity, 2) fossil content and conditions, 3) character of sideritic material, when present, 4) mineral grain conditions, and 5) miscellaneous comments.

The mica-clay mineral fraction is of significant value in evaluating depositional processes and diagenetic history. X-ray diffraction analyses were performed on many samples throughout the Hackett Section (See figure 4), most of which were conducted to investigate the character of the sideritic material. Clay mineral content was also examined for selected samples taken from the various thin-shale intervals in the Hackett Section. Table 4 shows the samples (and units represented) that were run in the low 2Θrange.

Table 4*

SAMPLE LOCATION OF X-RAY DIFFRACTION ANALYSIS OF SELECTED HACKETT SHALES

Sample #	Unit
HAGS - 9	17
H - 10A	16
HAGS - 4	6
H - 3	4
H - 1	3
HAGS - 1	2

*For detailed sample location see Figure 4

Table 4. Sample Location of X-Ray Diffraction Analysis of Selected of Hackett Shales.

All samples were machine-ground by a spec-mixer for a period of 20 minutes and then passed through an 80 mesh. A small aluminum holder with a rectangular reservoir was used. The sample was lightly tamped with a spatula until a flat surface was obtained, avoiding severe orientation of the platy minerals. However, using this method does not result in a strictly unoriented sample (not even possible), although it does allow for a sufficiently unoriented sample to get hkl diffractions, which were clearly evident in the diffractograms. A copper tube with nickel filter was employed for all X-ray analyses. Chart speed varied depending on objectives; 1°2Θ, 2°2Θ, and 2.25°2Θ per minute were used.

Kaolinite (7Å), illite (10Å) and some chlorite-type (14Å) structures were identified by their basal spacings (001) in the shale samples run. Siderite was also found in some of the shale samples. Quartz is ubiquitous in all samples. One sample of the lower interval (from Unit 4) and one sample from a black shale unit from an outcrop at the intersection of U.S. 71 and State Route #10 approximately 4 miles east of the Hackett Section were heat treated at 600°C for 1 hour and rerun, the latter sample being used as a "baseline" for a "typical" black shale. Table 5 shows the results of the heat treatment.

Table 5

X-RAY DIFFRACTION ANALYSIS AND HEAT TREATMENT OF SELECTED HACKETT SHALES

	d spacing Å		
Sample H - 3	K	I	Ch
No Heat	7.13	10.07	14.37
60°C (1 hr)	7.15	10.05	14.31
600°C(1 hr)	No peak	10.03	14.21
Sample 71-10A			
No Heat	7.17	10.03	14.35
60°C (1 hr)	7.17	10.01	14.30
600°C(1 hr)	No peak	10.16	14.14

Table 5. X-Ray Diffraction Analysis and Heat Treatment of Selected Hackett Shales

Sample H-3 is from a predominantly black shale unit. However, the sample is black carbonaceous shale with finely interlaminated red shale. A pre-heat treatment diffractogram also indicates a possible 3.54Å chamosite peak. Upon heat

treatment both the 7Å and the 3.54Å peaks were destroyed which suggests that chamosite with a kaolinite-type structure may be present in the sample. Chlorite (14Å) did not intensify but did significantly contract. Carroll [22,23] indicates that chamosite usually has a very disordered crystalline structure and can occur either as a disordered kaolinite-type structure or as a chlorite-type structure. Since the chlorite peak is not well developed and did not intensify upon heating (as do chlorite-type chamosites), a kaolinite-type structure of chamosite was indicated, that is, if chamosite exists at all, since chamosite does not usually produce hkl peaks because of its characteristic disordered crystalline character. It is clear that a chlorite-type chamosite is not present. The question must remain open regarding the presence of chamosite. Kaolinite is probably the dominant 7Å mineral present.

Illite (10Å) appears to be predominantly a 2M muscovite type which differs from most illites where lMd polytype is common [24]. That some disorder in the illite structure is suggested by the contraction under heating, probably expelling water layers. Hkl peaks of the 2M poly type are numerous. A 2.55Å peak of the lMd polytype is evident.

Chlorite is of very low abundance and/or very poorly crystallized. When detected, it shows a poorly diffused peak near 14Å. Heating did not affect the structure in intensity but does significantly contract the structure. It should be noted that sample 71-l0A also contained siderite. It obviously is not a "typical" black shale and interpretations based on the Hackett section have some possible implications to the interval from which sample 71-l0A was taken.

In going up the section, the lowest sample, HAGS-1 shows a well developed 7Å and 3.54Å (kaolinite structure) and a sharp 10Å illite-based peak, accompanied by a 2.55Åhkl. Chlorite is indicated by a sharp but very low intensity peak. Siderite and quartz are also present.

Sample H-1 is similar to the above in clay-mineral content. Siderite was, however, not indicated. H-3 has been discussed previously. HAGS-4 is also similar to the shales below, siderite being detected in this sample. HAGS-9 is also similar but the kaolinite and illite peaks are very well developed. Siderite may be present but is not clearly developed in the pattern.

The shales of Hackett Section appear to have rather uniform mineralogical characteristics. The kaolinite-type clay mineral structures and the illite-types approximate a 1:1 peak intensity relationship, with the chlorite-type always at very low peak intensities. Illite is clearly a mixture of 2M and lMd polytypes of muscovite with the possibility that the lMd is authigenic after the feldspars, which is evident in thin-section. The 2M polytype is usually detrital, which is also obvious in hand specimens.

Mineralogical character-Pocola section

As with Hackett section samples, estimates were made of the mineral species abundance (See table 6). A brief description of the thin-sections is also given in Appendix B. The sandstone units also consist of essentially quartz arenites.

Clay mineral content and character were examined via X-ray diffraction on selected shale samples. Table 7 shows the heat treatment analysis to which two Pocola shale samples were subjected. Sample PAPS-1 (Unit 23 - some 60 feet below Unit 26 and the first bedded siderite zone) shows strongly developed 7 Å and 10 Å peaks, with 14 Å absent. With heat treatment the 7 Å (and 3.54 Å) structures expanded slightly and then collapsed.

Table 6

POCOLA MINERAL IDENTIFICATION AND ABUNDANCE ESTIMATION

Fe Zone	Type	Sample#	Percent[1] Heavy Min.	Qtz & Chert	Calcite	Clay Min.	Micas	Plag.	RF
IX	III	PA-4	< 1	80	5	10	3	2	< 1
IX	III	P-12	< 1	85	4	10	3	1	< 1
*		DP-16	< 1	80	1	15	2	2	< 1
IV	I	P-6	< 1	80	2	10	6	2	< 1
*		P-7	< 1	80	2	10	6	2	< 1
*		KM1-13	< 1	80	2	10	2	1	< 1
III	I	P-51	< 1	80	2	10	2	1	< 1
II	I	P-4	< 1	80	2	10	2	1	< 1
*		DP-17	< 1	75	2	15	2	1	< 1
I	I	P-1A	< 1	85	2	7	1	5	< 1
*		KM1-11	< 1	80	3	10	< 1	5	2
*		KM1-20	2	85	1	6	< 1	2	3
		Ave.	< 1	80.8	2.3	10.2	2.5	2.1	< 1

[1] All counts excluded Fe material (multiple field of view averaging)
* Indicates interval from which sample was taken is not associated with a siderite zone

Table 6. Pocola Mineral Identification and Abundance Estimation.

Table 7

SELECTED POCOLA SHALE LAMINAE

Sample #	Kaolinite-Type	Illite d(Å)	Chlorite-type
PAPS-1			
No Heat	7.09	10.00	N.D.
60°C (1 hr)	7.16	10.01	N.D.
600°C(1 hr)	No peak	10.05	N.D.
P-6			
No Heat	7.12	10.03	14.44
60°C (1 hr)	7.16	10.07	14.26
600°C(1 hr)	No peak	10.05	13.72

Table 7. Selected Pocola Shale Laminate.

The l0Å structure expanded slightly upon heating and the 2M muscovite component's 025 hkl and 004 hkl intensified. Siderite is present and identified by its 2.79 Å and 3.59 Å peaks that were sharp but with heat treatment both collapsed. The shale is reddish brown to purple in color. Chlorite is absent.

Sample P-6, a black shale laminae (from siderite Zone IV of Unit 29) shows very well developed 7 Å and 10 Å peaks, the latter of slightly greater intensity. A small, but clearly evident 14 Å peak was present.

Illite-muscovite associated hkl are very well pronounced both before and after heating, the 025 hkl at 2.99 Å is not well-developed, as in sample PAPS-1. A straight expansion and contraction phase was experienced by the illite suggesting mixed polytypes are present; Both the kaolinite-structures 7 Å and 3.54 Å peaks expanded and then collapsed after heating. Chlorite contracted considerably and intensified slightly, probably indicating that disordered forms are present, perhaps some chlorite-type chamosite in this case. Siderite was, however, not detected in this sample.

Mineralogical comparisons: Hackett and Pocola sections

Similarities in mineral content between the Pocola and Hackett Sections might be anticipated. A slight increase,

however, in plagioclase abundance was noted in the Pocola Section. Units 17 and 18 of the Pocola Section show a higher abundance of metamorphic rock fragments and heavy minerals. Sample KMI-20 contains approximately 2% of heavy minerals consisting of two varieties of zircon (i.e. rounded and euhedral) and tourmaline. Alteration of feldspars, clay mineral content as indicated from thin-section, quartz characteristics, etc. are essentially identical, suggesting a common source for both Pocola and Hackett sediments.

The shales of the Pocola Section exhibit similarities to those at Hackett. One noticeable difference is in sample P-6 which showed a chamosite character to the chlorite shift and intensification under heating. Another feature of the Pocola shale series analysis is that most shales, if not all having color hues near red, contain a significant siderite component (Type II-A siderite). This indicates erosion and redistribution of pre-existing siderite or the formation of siderite within some shale units and not others. A biologic influence is suggested for the latter process, a feature that will be explored later.

Siderite Zones

Preliminary statement

The lithological (textural and mineralogical) characteristics of the sediments associated within the siderite zones have been described. Based these features, and as will be discussed further, the primary controls for the formation of the zones containing siderite were likely either physic-chemical or biologic in character. Either fecal matter (organic-rich) or iron (as a colloid or in suspension) was concentrated by gentle bottom currents, with time becoming a viscous, possibly calcareous mud. Siderite is common in some soil types [25].

The initial impression of the subject sediments, based solely on the physical characteristics of the depositional environment, is that syndiagenetic alteration of organic-rich material via microbial activity likely produced organic-rich pyrite precursors where sulfate reduction did not reach completion, or where organic-rich siderite forming in masses where sulfate reduction was either inhibited or reached completion, followed after burial by the introduction of Fe^{+2}-rich groundwater [26]. The original iron-rich or organic mud remained undisturbed where erosion did not occur, e.g. troughs of ripple marks, etc., where erosion did disturb the original fine-grained detritus (mud) by reworking and transport of the mud fragments via minor and major distributary sand channels occurred. Redistribution via solution and precipitation of siderite may have also occurred simultaneously in the porous media within the near-surface of the sediment associated with the iron and/or organic-rich zones, limited only by abundance of bottom dwelling fauna and the rate at which the resulting bioturbation and anaerobes promoted sulfate reduction.

A "siderizing" geochemical environmentlikely supplied the zones with Fe^{+2}-rich groundwater from nearby coal-forming swamps located up the hydraulic gradient [26] (see "General Stratigraphy"). Some calcareous materials present within the sediment were partly to fully replace by siderite. The calcite contained within certain faunal groups, however, was sufficiently dense to avoid the "siderization" process.

Certain types of siderite occurrences to be discussed later indicate that the organic or iron-rich mud escaped erosion, while other types are the result of erosion, either physical redistribution at the original depositional surface or chemical redistribution via solution and reprecipitation in the subsurface. The former would depend upon bottom current velocities, distributary channels and sedimentation rate, while the latter would depend on the rate of movement and chemical make-up of the siderizing solution cell.

To provide additional insight into the siderization process, a detailed description was developed for the siderite zones based on field descriptions and on microscopic analysis, with emphasis on the lithological, textural and mineralogical characteristics of the enclosing sediments. Table 8 is a tentative classification and general description of the siderite occurrences developed for the Hackett and Pocola Sections. The relative frequency of occurrence of the various siderite types in the two sections is also given.

The bedded types of siderite (Type I, II, etc,) have been generally classified as "blackband" or "clayband" siderite [27], and are typically associated with coal beds, notably of Carboniferous or Permian age. The "blackband" variety of siderite is significantly higher in carbon or organic content than the "clayband" siderite.

Hackett Section-Occurrences

Siderite type I: The Hackett Section contains seven of the eight types of sideritic zones defined in table 8. Type I, the most common type, is a massive reddish-brown (G.S.A. Color Code: 5R2/3), fresh variety (SGY4/l), occupying troughs of ripple-bedded and bioturbated, fine-grained sandstone. The zones are a maximum of ½ to 1 inch in thickness and extend only six to ten feet laterally. This type often grades into rather continuous dark gray shale laminae, which is also discontinuous, but extending over a greater distance than the sideritic zones.

Low-angle cross-bedding is occasionally apparent within some sideritic occurrences of Type I and flaser bedding is always apparent. Burrow structures are associated with the sandstones containing Type I zones, as with most other types. Burrows are, however, also common in non-sideritic intervals.

The significant features of Type I zones and selected sampling sites at the Hackett Section are illustrated in figure 17. Figure 17A (within Figure 17) shows the flaser bedding and burrows without siderite fillings. Figure 17B illustrates a Type I occurrence and a Type III fossil debris zone. The reddish color of all Type I occurrences is a weathering phenomenon, forming as a thin patina around fresh, dark gray to black, massive siderite (5GY4/1). Of special note, however, is that hematite, geothite, or limonite were not detected in the X-ray diffraction patterns, probably being either below that technique's detection limit or being amorphous in character.

Table 8

TENTATIVE CLASSIFICATION OF SIDERITE OCCURRENCES IN HACKETT AND POCOLA SECTIONS

Relative Frequency of Occurrence	Siderite Type	Characteristics	Reference Figures (F) Tables (T)
1	I	Reddish-brown to dull gray and massive occurring on upper surfaces of ripple-marked sandstone beds (thickness ½" to 1")Flaser bedding relationship with underlying sandstones.	F.8,14,17, 27,28,31, 32,33,34, 36,46 T.9,10,3,6
3	II	Black, massive and associated with very thin,highly carbonaceous and micaceous shale partings and laminae.Similar to Type I.Also occurs on upper surfaces of ripple-marked sandstone and associated with flaser bedding(thickness:½" to 1")	F.46 T.9,10
5	II-A	Reddish-brown partings and laminae, associated with very thin,highly carbonaceous and micaceous shale partings and laminae and dark gray shale (thickness: laminae only)	F.27,44 T.9,10
2	III	Brown to reddish-brown fossil debris, with large fossil fragments of pelecypods, gastropods, brachiopods and echinoderm plates and spines,partially to completely replaced by siderite.May be massive or thin coherent stringers of fossiliferous fragments.Siderite mud in part.May also contain carbonaceous fragments or laminae.	F.7,17,34, 38,39,45, 47,49,50, 51,52,53, 54,55,56, 57,58 T.3,5,6,9, 10,11
4	III-A	Reddish-brown,thin bands(less than 1cm) and burrows filled with siderite mud. Strongly bioturbated in part with scattered echinoid plates only.	F.18,19,21, 22,23,24, 29,30,34, 37,43, T.6,7,10
6	IV	Clasts, rounded, found in cross-bedded structures and relatively massive stratigraphic units. Size:up to 1" diameter.	F.14,17,25 26,40
7	IV-A	Ferruginous banding containing siderite in pore spaces of dark brown sandstone. Is usually associated with planar bedding. Small euhedral crystals.	F.11,12,13 41,42
8	V	Nodules,round or ellipsoidally massive reddish-brown to dull gray internally, associated with Type II and II-A and carbonaceous,micaceous shale partings and laminae.Max.size:4.5cm X 8.0cm X 2cm thick.	

Rank: 1 - highest recorded frequency in Pocola and Hackett Sections
7 - lowest recorded frequency in Pocola and Hackett Sections

Table 8. Tentative Classification of Siderite Occurrences in Hackett and Pocola Sections.

Additionally, striations (slickensides) were noted on the upper surface of the massive Type I siderite zones, parallel to bedding in one plane as well as discordant to bedding in other locations. Thrust faulting has been reported in the Pocola Section [4] (Orientation of these slickensides was observed to be generally north-south, but variations of up to ± 10° were recorded. This indicates that post-depositional movement of overlying rocks over the siderite might have served as thrust or growth faulting planes, locally or more widespread, as individual sheets or as block sheets with multiple zones of weakness (along thin but well-developed siderite zones?).

The Hackett Section shows Type I siderite in Zones, I, III, IV, V, VI, and VII (See figure 17). All figures show zones, sample locations, type of siderite and the data for each sample available.

Siderite type II: Type II is similar to Type I in being massive, with occasional low-angle cross-bedding persisting through the material; it is always associated with burrowing. Type II differs from Type I in color in being characteristically black and always associated with highly carbonaceous and micaceous silty sandstone with thin (less than 5 mm) stringers of coaly material.

Siderite type II-A: This type is predominantly sideritic shale (l0R4/n) and is often, although not exclusively, associated with carbonaceous, micaceous silty dark gray sandstone and shale and with Type I. Type II occurs in Zone I, II and III of the Hackett Section.

Siderite type III: This type, the second most abundant type, is predominantly a fossiliferous zone. Burrows are always present, some filled with ferruginous material, some not. Figures 18 and 19 show the typical character of burrows, both filled with sideritic material and without sideritic material. The former exhibits deformation of burrow (from compaction siderite mud?), the later remains circular (resulting from support provided by quartz grains?).

Fossil material present in Type III occurrences are highly disarticulated and fragmental. A few gastropods, pelecypods, numerous echinoid plates and spines and crinoid plates and columnals were noted along discontinuous stringers in the sandstone. The zone is characteristically light brown in color. Figures 6 and 7 also show Type III occurrences. Note banding marked by rock hammer. These sands are calcareous and sideritic, with fossil fragments partly to totally replaced by siderite.

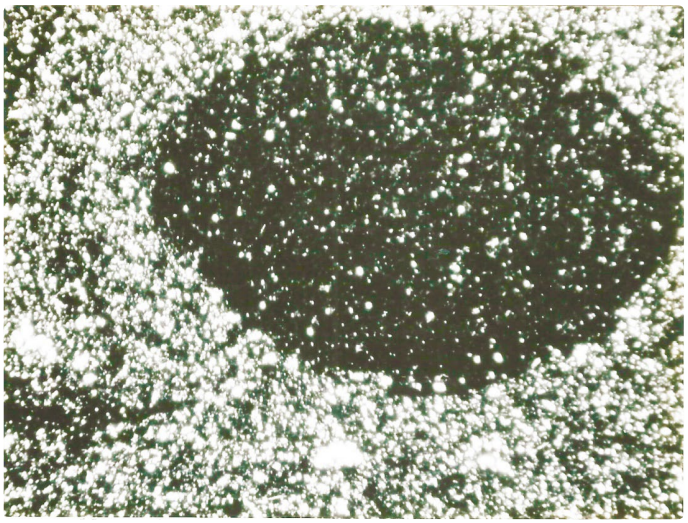

Figure 18. Hackett Section: Photomicrograph of Burrow Filled with Sideritic Mud (associated with Type III-A Siderite Zone I). 4X, Plane Light, Sample HA-14.

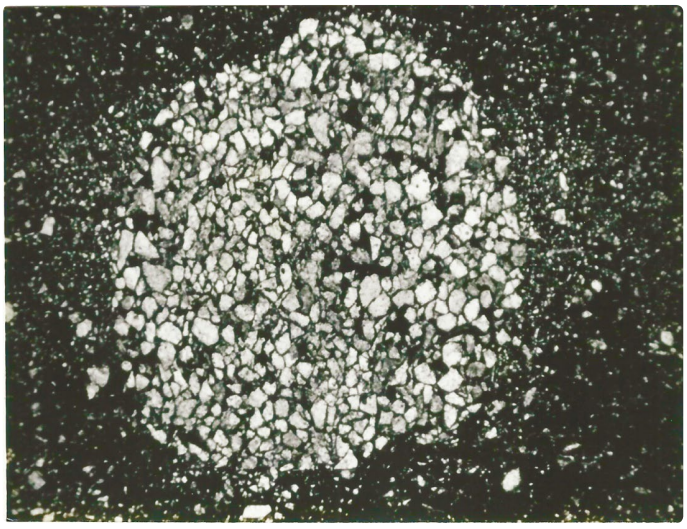

Figure 19. Hackett Section: Photomicrograph of Burrow Filled with Quartz Grains Surrounded by Sideritic Mud (associated with Type III-A Siderite Zone I). 4X, Plane Light, Sample HA-14.

Siderite type III-A: This, sub-type of Type III is characterized by rather massive, but very thin sideritic zones with common echinoid plates and spines (See figures 20 and 21) and disturbed bedding involving heavily burrowed sideritic laminae.

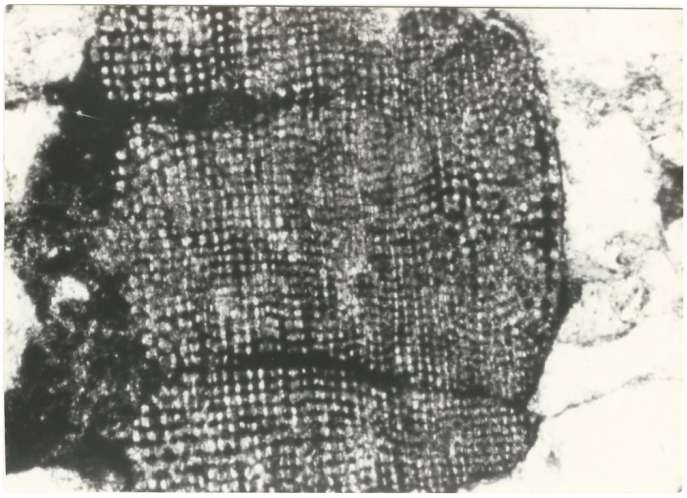

Figure 20. Hackett Section: Photomicrograph of Echinoid Plate Showing Siderite Replacement of Calcite. Siderite Zone VII. Sample H-50B, 40X, Plane Light.

Figure 21. Hackett Section: Photomicrograph of Echinoid Platesand Fossil Fragments within Burrow. Type II-A (laminae). Siderite Zone I. Sample HA-13, 10X, Plane Light.

Figures 22 and 23 are a typical example of disrupted bedding involving the sideritic laminae (dark color) as a result of burrowing. A typical burrow associated with siderite laminae (Type III-A) is shown in figure 24. Note orientation of platy intervals. Type III occurs in Zones I, II, III, and VII.

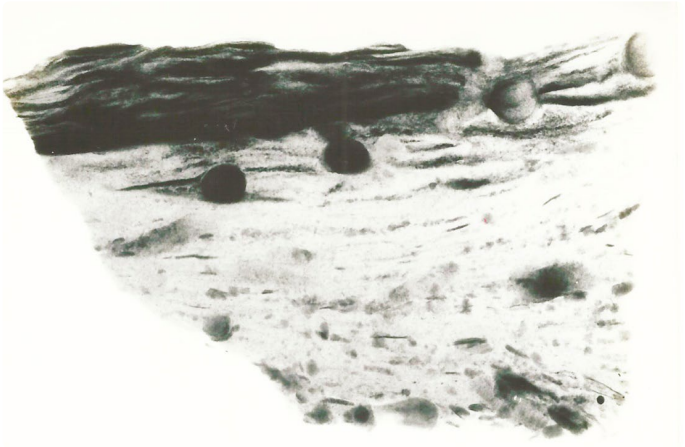

Figure 22. Hackett Section: X-Ray Photograph. Type III-A Siderite Zone II. The Dark Areas are Sideritic. 1X, Sample HA-2.

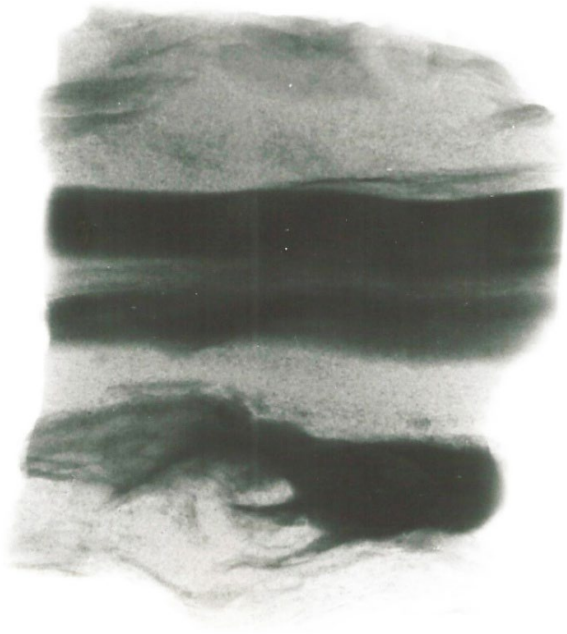

Figure 23. Hackett Section: X-Ray Photograph. Type III-A Siderite Zone VII. The Dark Areas are Sideritic. 1X, Sample H-50**.**

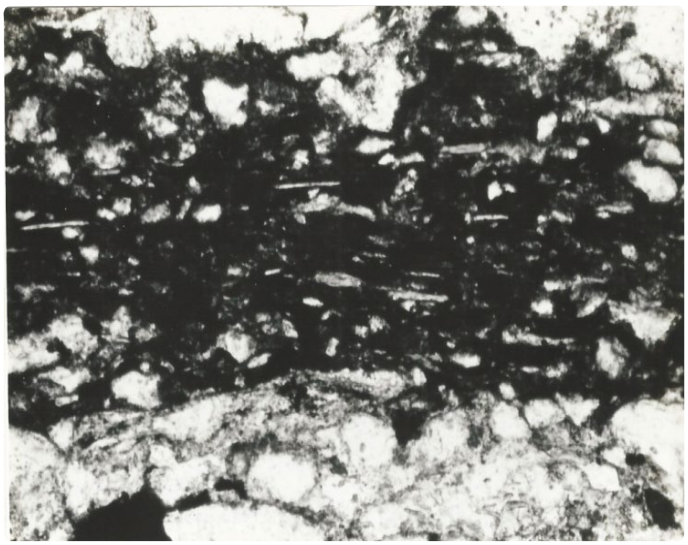

Figure 24. Hackett Section: Photomicrograph of Type III-A Siderite Zone VII. The Dark Areas are Sideritic. 4X, Sample H-50B.

Siderite type IV: Type IV is composed of isolated siderite clasts. This type occurs just above Zone I, just above Zone VI and as Zone VIII of the Hackett Section. All but Zone VIII are within a few vertical feet of Type I occurrences. Figure 25 is a photomicrograph of one of the clasts. Note the size and orientation of the dark material. Clasts (color: 10R3/4) are ellipsoidal to rounded and range in size from less than 0.5 cm at the long axis to 1 inch. Most are rounded; some are angular with long axis parallel to apparent bedding. In certain samples, gray shale clasts associated with discontinuous gray, carbonaceous laminae extend for only a few centimeters. Isolated echinoid plates are present.

Of note in the photomicrograph of figure 25 is that the upper boundary of the clast is relatively smooth whereas the lower boundary has an irregular contact with underlying quartz grains, suggesting that the material was soft when deposited and compaction has compressed the clast out of round.

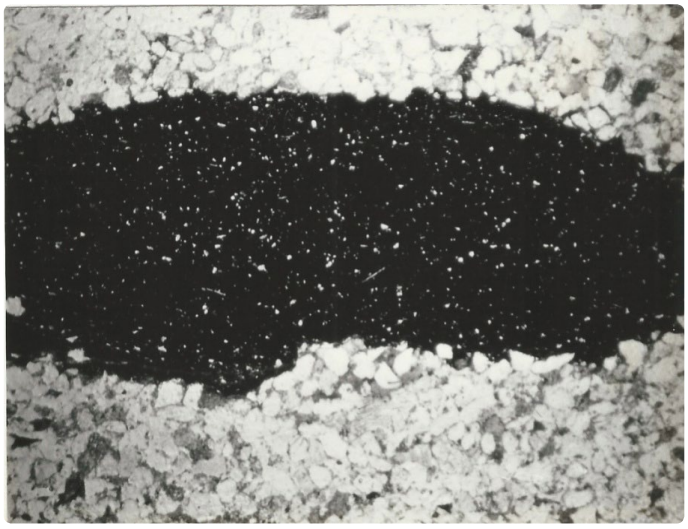

Figure 25. Hackett Section: Photomicrograph of Siderite Clast, Type IV, Zone VII. The Dark Areas are Sideritic. 4X, Sample H-14.

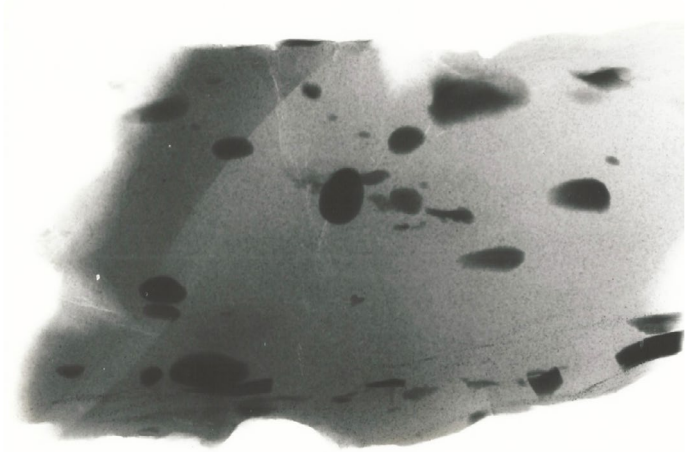

Figure 26. Illustrates the Clasts in Zone VIII of the Hackett Section.

Siderite type V: The only occurrence of Type V nodules is in Zone III where three large nodules were recovered from coaly, highly mica-ceous, dark silty sandstone. Trilobite fragments were recovered in the bed containing the nodules (Faunal descriptions will follow). The largest ellipsoidal nodule measured 4.5 cm × 8.0 cm × 2 cm thick. Others were round with diameters of approximately 6 cm and the orientation of the long axis was north-south relative to the Hackett Section. Some affinity of Type V with Type II-A is apparent, because of their association, but nodular occurrences are unique and are limited to Zone III at the Hackett Section.

Pocola section-Occurrences

The Pocola Section contains essentially the similar types of siderite occurrences as defined in table 8 and described for the Hackett Section. However, some variations do occur in the Pocola Section. Figure 27 is a detail section of Zones I, II and III, showing typical occurrences of the zone types.

Type I Siderite: The typical occurrence of Type I siderite is shown in figure 28. Type I occurrences dominate Zones I through III in the Pocola Section but are less continuous laterally than Type I of the Hackett Section. Figure 27-D illustrates an occurrence of pyrite recorded between the two zones. Note the relationship of the burrowing structures, indicating pyrite may have replaced organic material. The sandstone enclosing the pyrite is very siliceous with considerable quartz overgrowths. The pyrite is heavily weathered but appears to be very fine grained. Pyrite is also recorded in Type I was very fine, euhedral grains within a circular, horizontal burrow, suggesting that pyrite may be a precursor to siderite, under some conditions.

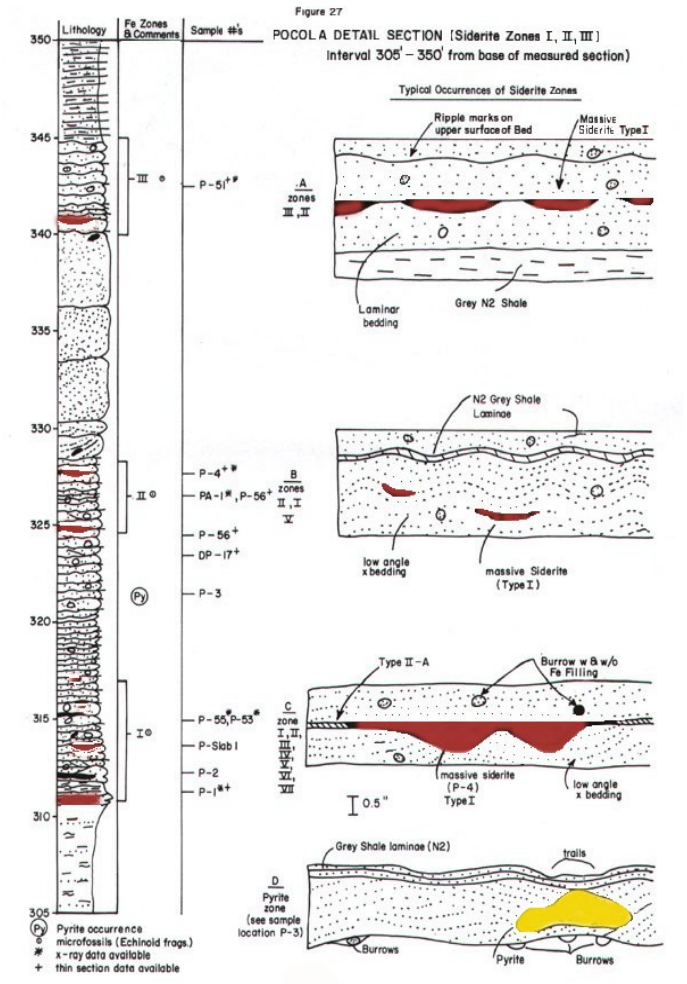

Figure 27. Pocola A Detail Section [Siderite Zones I, II, III] Interval 305'-350' from base of measured section.

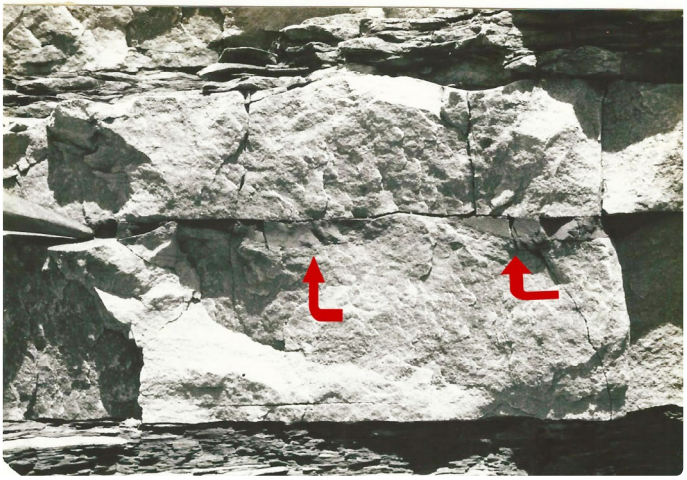

Figure 28. Pocola Section: Outcrop Close-Up View of Type I Siderite Zone 1. Note that Type I Occupies Ripple Troughs.

In the same zones, Type III-A occurrences are also numerous and show the strongly bioturbated character of the sediment involving the sideritic material (See figures 29 and 30).

Figure 29. Pocola Section: X-Ray Image of Type I Siderite Zone I (top) and Disturbed Siderite Bed at Bottom (Type III-A) 1X Sample P-1A.

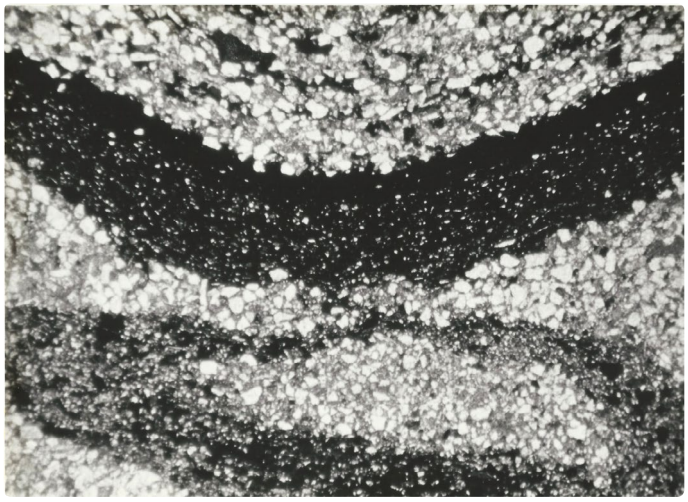

Figure 30. Pocola Section: Photomicrograph of Disturbed Bedding of Siderite. Note Compressed Burrow Below Sagging Siderite Band and "Partial Gravity Grading" of Quartz Grains within Siderite Band, Type III-A Siderite Zone III. 4X Plane Light, Sample P-51.

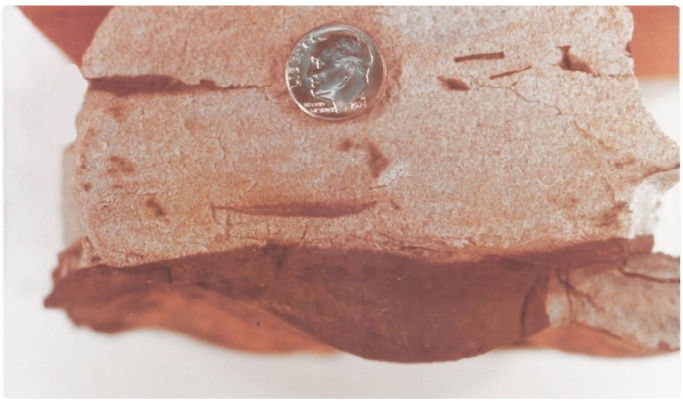

Figure 31. Pocola Section: Hand Sample View of Type I Siderite Zone II. Note Shape of Type I Occurrence of Clasts in Sandstone Above Type I Siderite Band Filling Ripple Marks. Sample P-4 (See figure 28).

Figure 31 illustrates in more detail Type I from Zone II. Note the ripple-marked character of the bottom of the dark sideritic material and the clasts and associated zones with curved bases just above the Type I. Figure 32 is a close-up view of the bottom of the zone shown in figure 31. Note the pock-marked texture. The texture does not appear to be quartz-grain impressions because the quartz grains are too small to fit into that texture. It may be due to pellets in the original mud. There is also a suggestion of slicken sides on the bottom of the Type I Siderite sample.

Figure 32. Pocola Section: Bottom of Above Hand Sample Shown in Above Figure 31. A Type I Siderite Zone II. Note Bottom as Pock-Marked with Suggestion of Slickensides.

Figure 33 is an X-ray image of a similar Type I occurrence in the same zone. Note the truncating sedimentary structure shown by the near-parallel lamination just above the dark material and the laminations parallel to the sideritic material.

Figure 33. Pocola Section: X-Ray Image of Type I Siderite Zone II. Note Truncating Depositional Structure of Low-Angle, Small-Scale Cross-Bedding with "Rip-Up" of Top of Type I Siderite band. Sample P-4.

Figure 34 (A-C) is the detail section for Zones IV through VIII, showing significant types of siderite zones. Figure 34A is the thickest siderite zone (VIII) in both the Hackett and Pocola Section (approximately four inches thick). Figure 35 is an X-ray photographic view of light gray sandstone with abundant burrowing structures and numerous shale laminae. Zone VII, illustrated in part by figure 34-B.

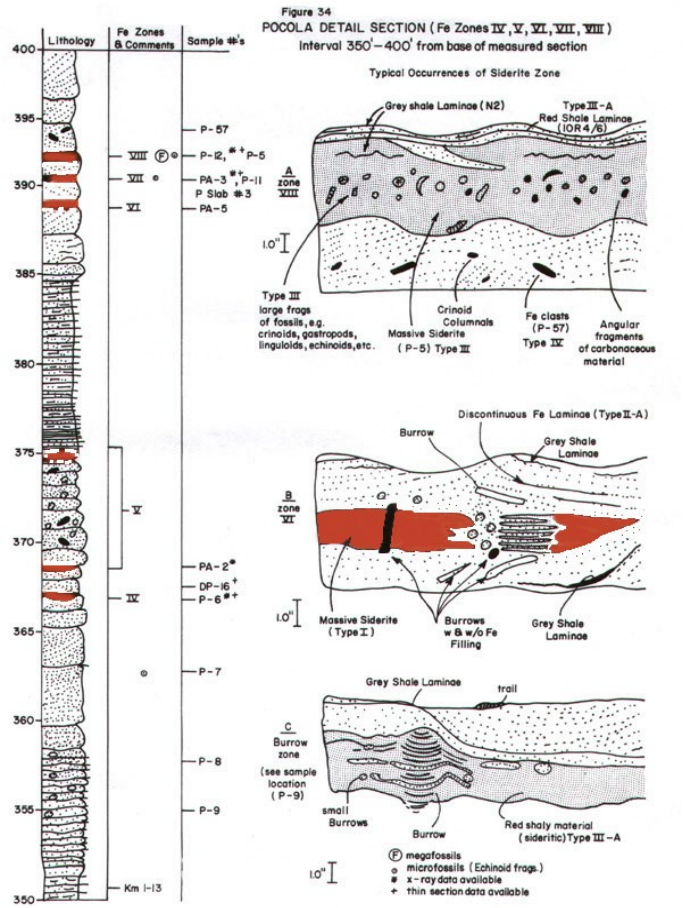

Figure 34. Pocola Detail Section (Fe Zones IV,V,VI,VII,VIII) Interval 350'-400' from base of measured section

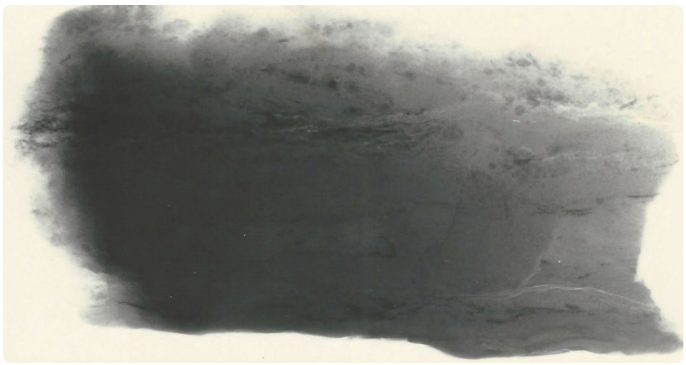

Figure 35. Pocola Section: X-Ray Image of Sample P-8 Showing Low-Angle Cross Bedding with Black Shale Laminae and Burrows. 1X

Figure 36. Pocola Section: Slab View of Type I Siderite Zone VI. Note Disruption of Type I Siderite Zone by Apparent Burrowing Activities. Zone is about 3 cm, in Thickness.

Figures 36 and 37, clearly shows sideritic material interrupted by burrowing activities.

Figure 37. Pocola Section: X-Ray Image of Sample P-5A. Note Apparent Disruption by Burrowing Activities in Type III-A Siderite Zone. 1X

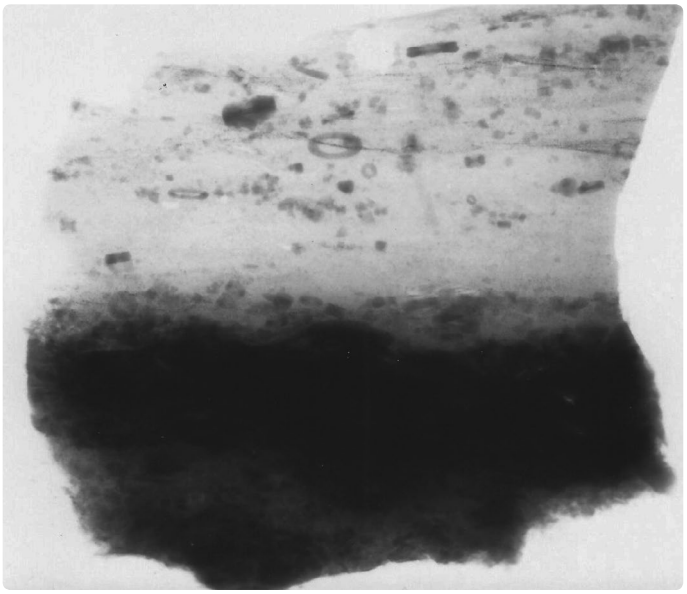

Figure 38. Pocola Section: X-Ray Image of Sample P-5. Note Apparent Disruption by Burrowing Activities in Type III-A Siderite Zone. 1X

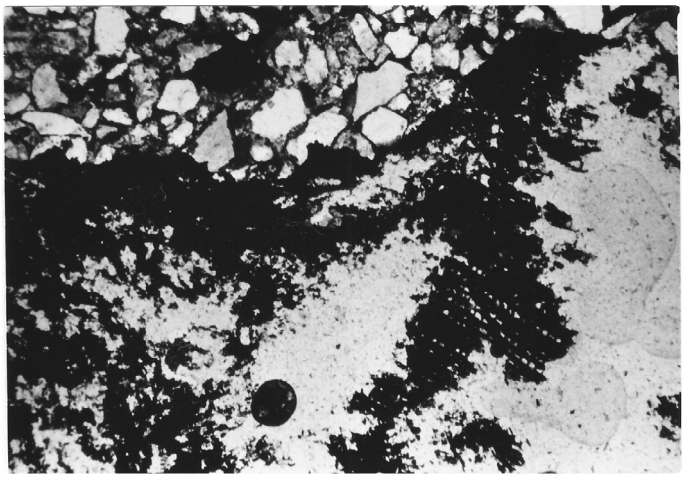

Figure 39. Pocola Section: Photomicrograph of Coal Fragment in Fossil Debris Zone (Siderite Zone VIII). 10X Plane Light, Sample P-12.

Zone VIII is a "fossil hash" zone (See figures 34A and 38). The dark zone is sideritic material. Zone VIII containing Type III comprises coaly laminae and large angular fragments of coaly material (See figure 39). Figure 40 illustrates the clasts and burrows above Zone VIII.

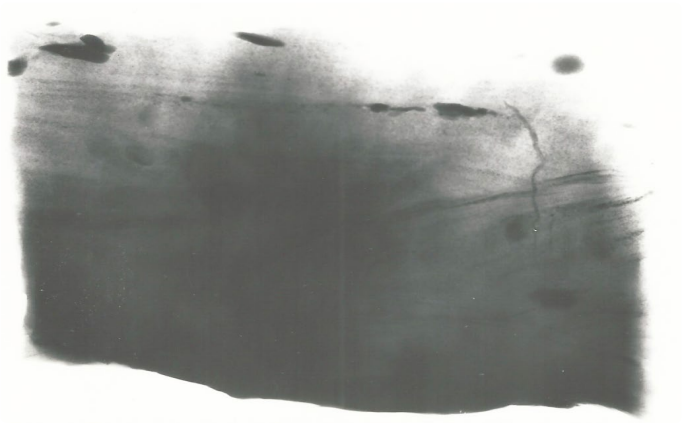

Figure 40. Pocola Section: X-Ray Image of Type IV (Clasts) above Siderite Zone VIII. Sample P-57. Note Clasts (Very Dark and Oblate), Burrows, and Low-Angle Cross-Bedding, 1X.

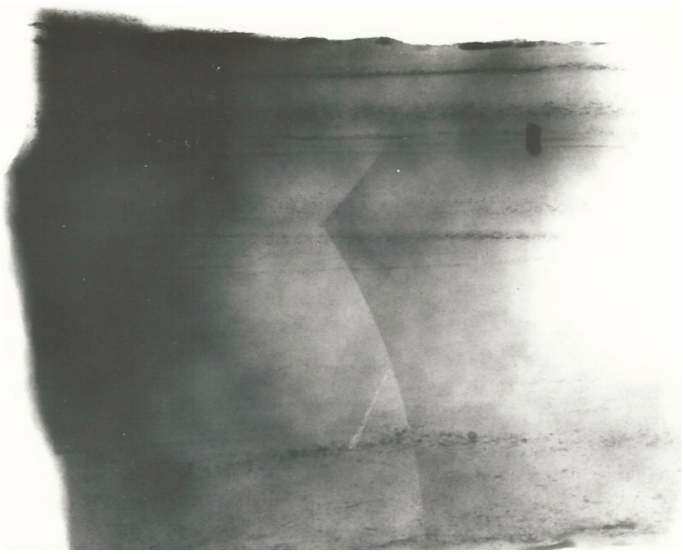

Figure 41. Pocola Section: X-Ray Image of Type IV-A (Clasts) Note Planar Bedding; Laminae with Very Small Sideritic Rhombohedral Crystals and Fossil Fragments (Echinoid Plates), all Replaced with Siderite. Sample PA-4, 1X.

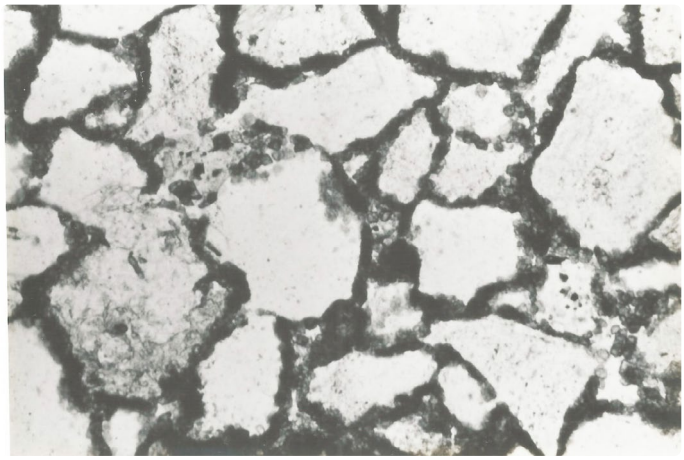

Figure 42. Pocola Section: Photomicrograph of Small Siderite Rombs Along Quartz-Grain Boundaries. Type IV-A Siderite Zone IX, 40X, Crossed Nichols, Sample PA-4.

Siderite Zone IX contains Type I and a type of occurrence not previously reported in the Hackett Section. Figure 41 above is an X-ray photograph of a sandstone bed containing ferruginous banding, as previously discussed, defined here as Type IV-A. The planar bedding contains numerous very small, sideritic, fossil fragments and small clasts (See figure 42 above). Figure 43 below is a photomicrograph of a Type III-A occurrence from Zone III. Note apparent "gravity grading" of quartz grains within sideritic material.

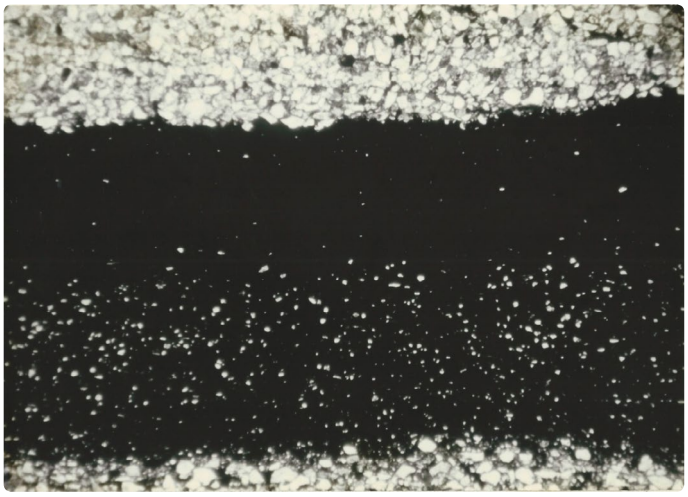

Figure 43. Pocola Section: Photomicrograph of Type III-A Siderite Zone III, 10X Plane Light. Note "Gravity Grading" of Quartz Grains Suspended within the Dark Siderite Band. Sample P-51.

Relationship of Siderite types

It is clear that the classification proposed in table 8 has a number of problems if applied rigorously. More than one type occurs within any one bed. For example, a Type I occurs at the base and top of Unit 5 in the Hackett Section. A Type III fossil debris occurs in the middle of the same unit. Further, a Type V occurs within Unit 9 at Hackett among carbonaceous, micaceous shale partings with Type II-A laminae. Type II black, massive siderite of one-half inch thickness occurs along the same major bedding plane some six feet away within a ripple-marked surface of light gray sandstone. In addition, Type I occurrences, when followed laterally, commonly grade into Type II-A laminae that are interlaminated with dark gray shale, without carbonaceous material.

In conclusion then, some types are interrelated; some are obviously related only in a genetic sense to other types. As previously mentioned in the introduction to this section, deposition, burrowing, erosion, reworking, disintegration and re deposition of the siderite or its precursor play a dominant role in forming the various morphologic types discussed above.

Mineralogy of Siderite zones

The X-ray diffraction data obtained from selected samples of the various siderite zones in the Hackett and Pocola Sections (See figures 4 and 9 for associated lithology) are summarized in tables 9 (for Hackett Section) and 10 (for Pocola Section). Measurements of d spacing were made relative to the 4.26 Å quartz peak present in all samples. Six samples were selected to serve as examples of the typical types of siderite occurrence as well as other minerals present in the various zones.

Table 9

X-RAY DIFFRACTION DATA ON SIDERITE ZONES - HACKETT SECTION

Fe Zone Occurrence	Sample #	Fe Type	Mineral Identified** Qtz[1]	Sid[2]	Cal[3]	Kaol[4] Type*	Ill[5]	Chl[6] Type*
VII	HA-13	Type I Fe (5R2/3)	D	D	C	--	C	--
VI	H-10B	Dk Gray SS w/ Type IIA 5R2/3 shale	D	M	ND	VM	VM	VM
V	HA-10B	Type I Fe (5R2/3)	C	D	VM	VM	VM	VM
	HA-12A	Type II Fe (Black)	C	D	ND	C	C	VM
	HA-12B	Type I Fe (5R2/3)	D	D	ND	C	C	VM
III	HA-4F	Type III Fe (Brown SS w/ fossil)	D	C	C	C	C	ND
	HA-4	Type II Fe (Black)	D	C	C	C	C	ND
	HA-3B	Type II Fe (Black)	D	C	VM	--	--	--
	HA-2	Type I Fe (5R2/3)	D	C	C	--	--	--
II	HA-1F	Type III Fe (Bn SS w/ Dis. Fossil Frags)	D	C	M	C	M	VM
	HA-14	Type II Fe (Black)	D	D	C	C	C	ND
I	H-4	Type III Fe (10YR6/2 w/ Dis. Fossil Frags)	D	C	C	ND	M	C

* Disordered chamosite indicated in some samples.
** Fe oxides resembling hematite, geothite, limonite, etc. not detected.
D = Dominant; C = Common; M - Minor; VM = Very Minor (Marginal Detection); ND = Not Detected; -- = Not Run

1
2 I.D. based on following peaks: 4.26Å(100), 3.34Å(101) plus other hkl
3 I.D. based on following peaks: 2.79Å(104), 3.59Å(110), 2.13Å(113) plus
4 I.D. based on following peaks: 3.04Å(104)
5 I.D. based on following peaks: 7Å(001), 3.54Å
I.D. based on following peaks: 1 Md polytype of muscovite: 10Å, 2.55Å; 2M muscovite: 10Å, 5.02Å, 4.48Å, 3.21Å
6 I.D. based on following peaks: 7Å and 14Å, plus hkl if present

Table 9. X-Ray Diffraction Data on Siderite Zones-Hackett Section

Figures 44 through 46 show X-ray diffractograms of the most commonly occurring siderite types. Most of the features mentioned above are illustrated by the various X-ray diffractograms.

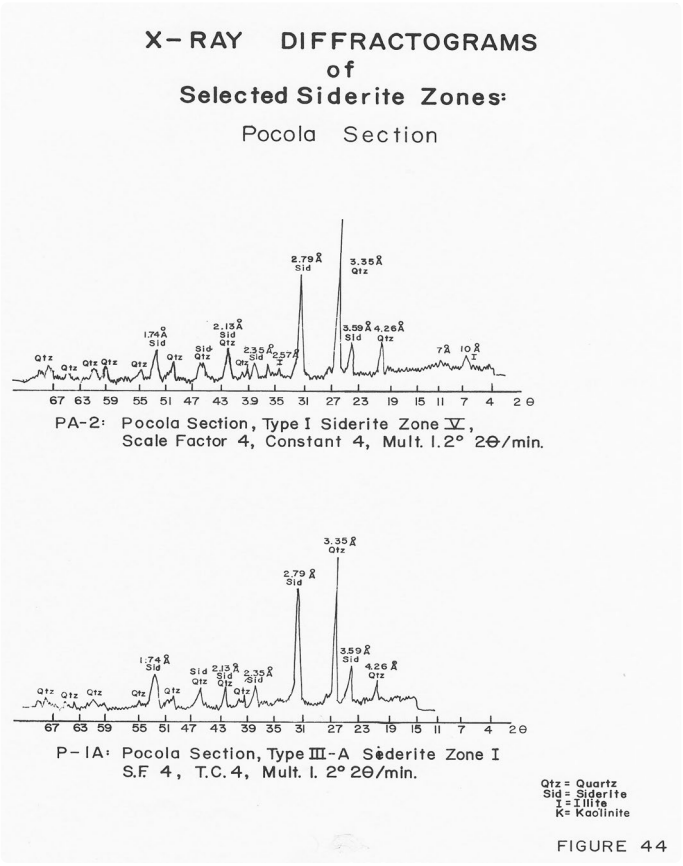

Figure 44. X-Ray Diffractograms of Selected Siderite Zones: Pocola Section.

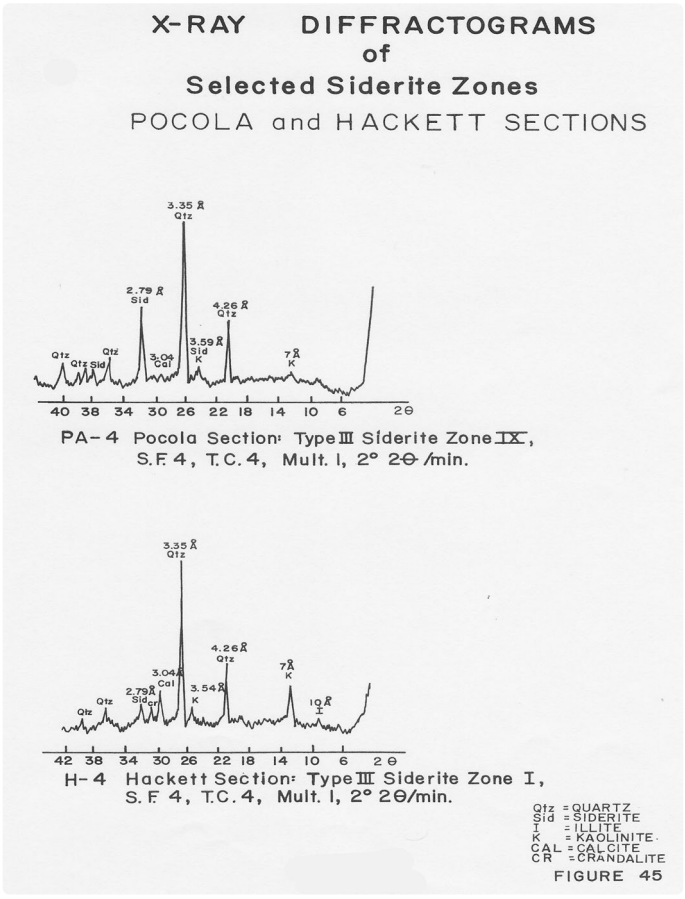

Figure 45. X-Ray Diffractograms of Selected Siderite Zones: Pocola and Hackett Sections

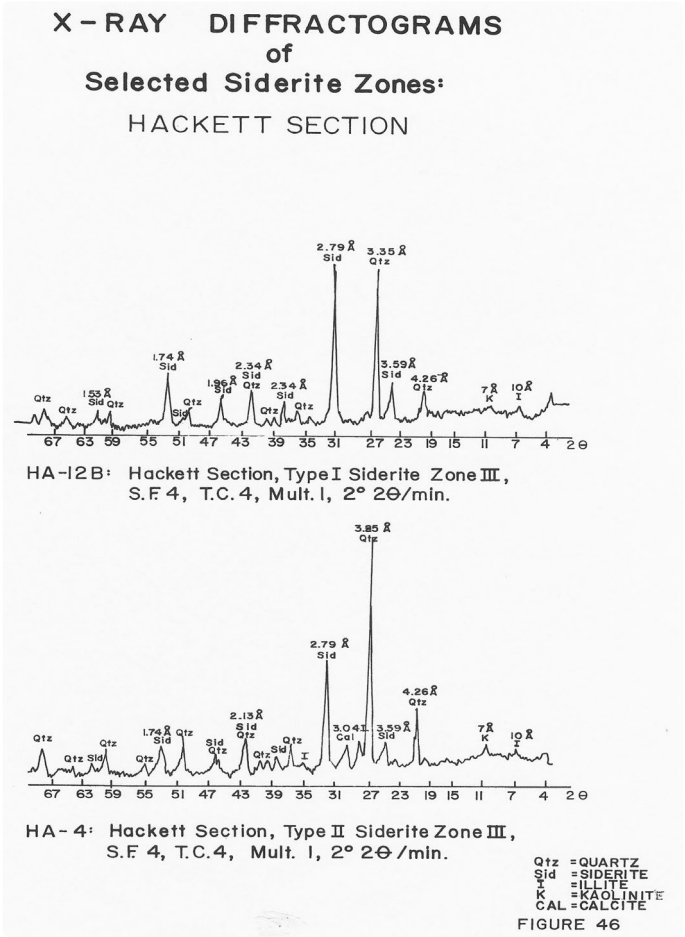

Figure 46. X-Ray Diffractograms of Selected Siderite Zones: Hackett Section

Siderite: The mineral siderite is the dominant iron mineral of the ferruginous zones. Peaks used for identification are shown in table 9. Based on the number of hkl shown, the siderite is crystallized, but cryptocrystalline in character because of its massive character. All material examined with a reddish to dark reddish brown color have a strong siderite component the interlaminated red shales (Type II-A) often interlaminated with black shale laminae have a dominant siderite component. Fossil material has also been replaced either partly or wholly by siderite and will be discussed later. See Peaks in figures 44-46.

Quartz: The mineral quartz is usually a co-dominant mineral with siderite within the siderite zones. Quartz invariably occurs as very fine detrital grains (See figure 43), floating within a matrix of sideritic material, often, but not always, showing a segregation of large grains in the lower part of the siderite band (within Type III-A especially).

Table 10

X-RAY DIFFRACTION DATA ON SIDERITE ZONES - POCOLA SECTION

Fe Zone Occurrence	Sample #	Fe Type	Mineral Identified** Qtz[1]	Sid[2]	Cal[3]	Kaol[4] Type*	Ill[5]	Chl[6] Type*
IX	PA-4	Type III Fe (Dis. Fossil Frags)	D	C	VM	VM	Vm	VM
	P-50	Type III Fe (Dis. Fossil Frags)	D	D	C	--	--	--
VIII	P-12	Type III Fe (Dis. Fossil Frags)	D	D	C	--	--	--
	P-5	Type III Fe (Dis. Fossil Frags)	D	D	C	M	M	VM
VII	PA-3	Type II Fe (Carbon)	D	D	VM	M	M	ND
V	PA-2	Type I Fe (5R2/3)	D	D	ND	M	M	VM
III	P-51	Type I Fe (5R2/3)	C	D	ND	--	--	--
II	P-4	Type I Fe (5R2/3)	C	D	ND	ND	ND	ND
	PA-1	Type I Fe (5R2/3)	D	D	ND	M	--	--
I	P-55	Type I Fe (5R2/3)	C	D	ND	M	--	--
	P-53	Type II Fe (Carbon w/ Red Laminae)	D	D	ND	ND	VM	ND
	P-1A	Type IIIA Fe (5R2/3)	D	D	ND	M	--	--

* Disordered chamosite indicated in some samples.
**Fe oxides resembling hematite, geothite, limonite, etc. not detected.
D = Dominant; C = Common; M = Minor; VM = Very Minor (Marginal Detection);
ND = Not Detected; -- = Not Run

[1] I.D. based on following peaks: 4.26Å(100), 3.34Å(101) plus other hkl
[2] I.D. based on following peaks: 2.79Å(104), 3.59Å(110), 2.13Å(113) plus
[3] I.D. based on following peaks: 3.04Å(104)
[4] I.D. based on following peaks: 7Å(001), 3.54Å
[5] I.D. based on following peaks: 1 Md polytype of muscovite: 10Å, 2.55Å; 2 M muscovite: 10Å, 5.02Å, 4.48Å, 3.21Å
[6] I.D. based on following peaks: 7Å and 14Å plus hkl if present

Table 10. X-Ray Diffractograms Data on Siderite Zones-Pocola Section

Calcite: The mineral calcite occurs in all siderite types, with a notable increase in Types III, III-A, and II reflecting the fossil material present.

Table 11

X-RAY DIFFRACTION ANALYSIS - HEAT TREATMENT
H-4 HACKETT SAMPLE (TYPE III SIDERITE ZONE I)

Sample H - 4	d spacing Å K	I	Ch
No Heat	7.04	10.05	14.14
600°C (1 hr)	7.09	9.99	13.92*

*Marginal detection

Table 11. X-Ray Diffraction Analysis-Heat Treatment H-4 Hackett Sample (Type III Siderite Zone I)

Kaolinite-Type Minerals: The identification of kaolinite within the various siderite zones are difficult because of the disordered character of the kaolinite structure. In general, Type III ("fossil hash" zones" show a pronounced 7 Å peak and a less developed 3.54 Å, suggesting. kaolinite, chlorite or chamosite. Heat treatment analysis of one Type III sample (i.e. sample H-4 from Zone I of the Hackett Section) is shown in table 11. Sample H-4 is a highly weathered fossil debris zone (Type III). Siderite is present as indicated by a low intensity 2.79 Å peak. Upon heating, the kaolinite-type structure expands and decreases in intensity slightly but does not collapse after heating. This characteristic indicates that a chamosite (chlorite-type) structure is present but the necessary increase in intensity as a result of heating of a 14Å peak is not present [23]. On the basis of the common association with siderite, however, a ferrous chamosite is indicated. All siderite samples X-rayed, show a very minor and poorly developed kaolinite-type component. An identification of kaolinite and chamosite is tentative but both are probably present in minor amounts.

Illite-Type minerals: Illite, although usually composed of the IMd polytype of muscovite, is a mixture of the authigenic IMd and detrital 2M polytypes of muscovite in the various siderite zones.

Chlorite-Type minerals: This mineral structure is present but not well developed in any of the siderite samples run, not detected in many. A special chlorite-polytype with a heat-resistant 7 Å structure is suggested as mentioned above (chamosite?).

Miscellaneous minerals: Plagioclase has been identified in almost all thin-section samples, in at least one of every type siderite occurrence. The identification is based on a 4.04 Å peak near the detection limit but is systematically present. Type III usually shows a 4.04 Å peak.

Crandalite, a radiogenic and oxidized phosphate mineral, has been tentatively identified in Type III samples by its characteristic well-developed 2.94 Å peak. Types I and II also may contain the mineral in very low quantities. Subsidiary hkl peaks are not present, probably because of its low abundance (See figure 45).

Fauna and flora of the Siderite zones

Siderite zones, when viewed in thin-section and in hand specimen, have significant faunal and floral components. Echinoderm plates and spines (both echinoids and crinoids), and pelecypods, brachiopods, trilobite fragments and numerous burrowing structures, tracks and trails have been recovered from the various siderite zones. Type III is characterized by the presence of "fossil hash".

Echinoids: Echinoid plates are very common to scattered in all siderite zones, either within cryptocrystalline siderite or in the non-sideritic sandstone above or below the sideritic material. They are notably absent in the intervals not associated with sideritic material (see brief thin-section descriptions in Appendix B). Plate fragments are a maximum of 2,0 mm across, with most of the plates smaller than 1 mm. Spines are of variable diameter; in cross-section they are a maximum of 20 mm.

Replacement of calcite by siderite in the echinoid fragments ranges from partial to complete. Most of the small fragments are totally replaced but in larger fragments the replacement is incomplete, with the high order calcite birefringence evident in thin-section. Siderite has a reddish color that obscures birefringence. The fine skeletal structure is still clearly evident. Figures 47 and 48 show typical echinoid fragments partly to completely replaced by sideritic material.

Figure 47. Pocola Section: Photomicrograph of Sample P-12. Part of Type III Siderite Zone III. Note the Rim of the large Echinoid Spine is Replaced by Siderite Whereas Interior Remains as Calcite. Fossil Fragments Accumulate Siderite–Organic? Material. Plane Light, 4X.

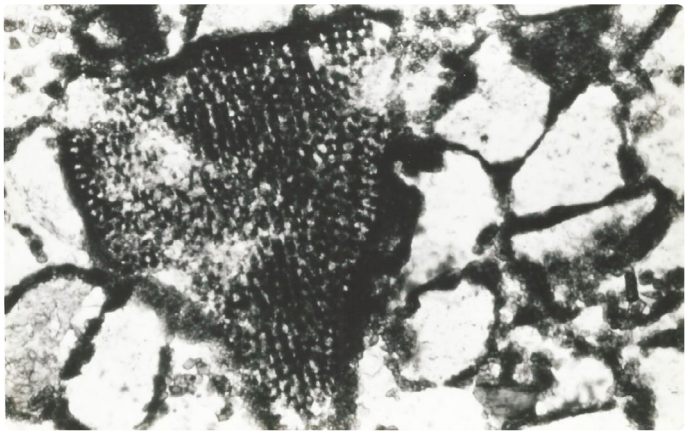

Figure 48. Pocola Section: Photomicrograph of Echinoid Fragment Almost Totally Replaced by Siderite Zone IX. Light Color on Echinoid is Calcite. Note small Siderite Crystals Along Quartz Grain Boundaries. Plane Light, 40 X. Sample PA-4.

Crinoids: Within the Type III siderite zones, which are characterized by fossil debris, numerous crinoid columnals and plates are present. They are apparently restricted to Type III zones, being conspicuously absent in the other types and zones.

The replacement character of the crinoid fragments is similar to that found in the echinoid fragments, Partial replacement of calcite by siderite is, however, the most common. Large columnals show only partial replacement whereas the smaller plates are totally replaced. Figures 49 and 50 show the typical replacement features of the crinoid material.

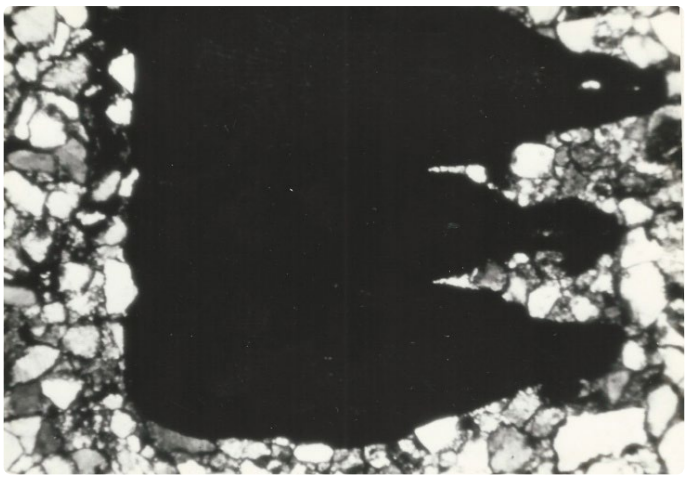

Figure 49. Pocola Section: Photomicrograph of Crinoid Plate from Siderite Zone VIII. Note Also, Small Siderite Crystals Along Quartz Grain Boundaries and in Interstices Between Grains. Crossed Nichols, 40 X. Sample P-12.

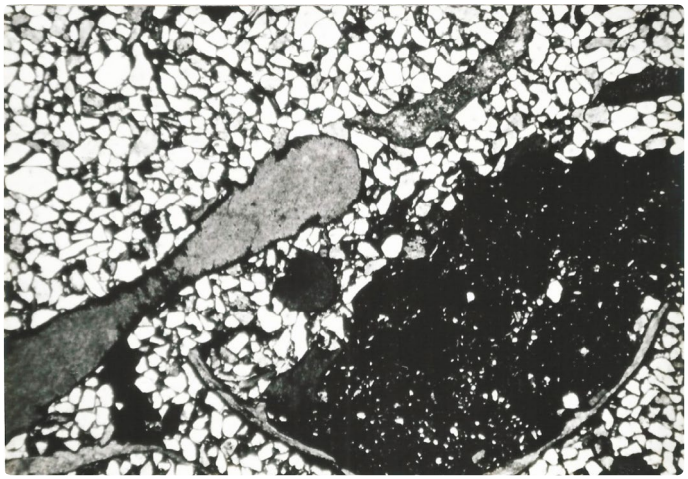

Figure 50. Pocola Section: Photomicrograph of Crinoid (Dumbbell Form). Echinoid Fragments and Segments of Pelecypods and Brachiopods in Type III Siderite Zone VIII. Sample P-12, 10X, Plane Light. Siderization Along Edges of Fragments and in Very Fine Grained Sediment-Organics. Now Replaced with Siderite.

Pelecypods: Some of the pelecypods show only very minor replacement but most have been essentially unaffected by siderite replacement. The calcite within the structures is usually prismatic and shows crystal orientation normal to the boundaries of the shell. Figure 51 shows a typical occurrence. Fragmental pelecypods are only recorded in Type III zonal occurrences in Units 5 and 7 of the Hackett Section and Unit 31 of the Pocola Section.

Figure 51. Pocola Section: Photomicrograph of Large Pelecypod Fragment Unaffected by Siderization, from Siderite Zone VIII. Sample P-12, 4X, Plane Light. Note Siderite Mud Blocked Pelecypod Fragment.

Brachiopods: Black, linguloid brachiopods were recovered from Zone VIII in Unit 31, among the massive "fossil hash" zone in the Pocola Section. These forms have phosphatic shells. Articulate forms were also recovered from Zone VIII, Unit 20, Zone II (Unit 7) and Zone I (Unit 5) in the Hackett Section. Figure 52 is a product id brachiopod. Note siderite-filled punctae. These forms have also not been affected by siderite replacement, but some are heavily weathered in outcrop.

Figure 52. Pocola Section: Photomicrograph of Brachiopod (Productid). Showing Punctae were Filled with Siderite. Dark Areas are Echinoid Fragments Replaced by Siderite. Sample P-12, 10X, Plane Light.

Trilobites: One specimen (a pygidium) was recovered from the Hackett Section (Zone III, Unit 9). It was associated with a siderite zone containing Types II, II-A and V. The color of the specimen is dark brown. Replacement by siderite is suggested. No other fossils were found in this interval. Trilobite fragments (genal spines) are reported in other fossil debris (Type III Zones). All fragments (the pygidium and the fragmental genal spines) compare favorably to *Kaskia* and *Paladin* of the Family Phillipsiidae [28].

Trace Fossils-Burrows: The siderite zones are often dominated by burrowing structures. Some burrows are filled with coarse grains than surrounding sediments, whereas some burrows are filled with fine grained sideritic material, of remarkable similarity to the internal structure and content of the thin horizontal sideritic bands.

Because of the present ambiguities involved in trace fossil classification, specific trace fossil forms were not investigated in any detail. Arenicolites, Chondrites, and Conostichus are common forms reported in the Hackett and Pocola Sections (K. Mc Millen, personal communication). Chamberlain [29] has reviewed the biogenic sedimentary structures of parts of the Arkoma Basin and Ouachita Mountains and reports Scolicia, Currolithes, Skolithos, Conostichus, Scaloarituba and arthorpod tracks from the Pocola Section. Based on those forms, he interpreted the depositional environment as tidal flats and nearshore marine. All small burrow cross-sections measured approximately 0.05 cm or less. The form Arenicolites is indicated by the individual U-shaped burrows recovered in some of the heavily burrowed intervals in both the Hackett and Pocola Section, noted by vertical and horizontal structures in Figures 4 and 9. These forms are most common in ripple-marked and low-angle, cross-bedded sandstone. Howard [30] described Arenicolites in some detail suggesting a shallow water habitat. Chondrites has been discussed by Simpson [31].

The form Conostichus (Figures 53 and 54) has been discussed by Branson [32], wherein many species were described from the Atoka Formation of Oklahoma. All the dark material shown in the above figures is slightly oxidized sideritic material. The surrounding sediment is clean without ferruginous material. Pfeffercorn [33], Chamberlain [34] and Fager [35] have examined Conostichus forms, the latter worker reporting recent structures with strong affinities to the Conostichus form. Fager's work suggests that it is related to the sea anemone burrowing structures found in a very shallow nearshore marine environment.

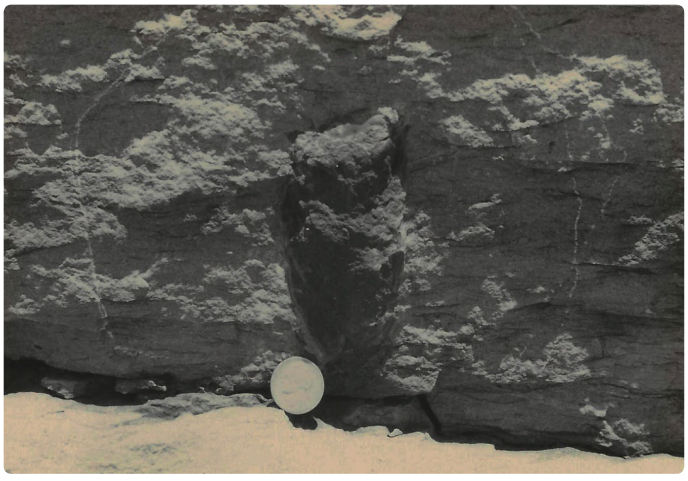

Figure 53. Pocola Section: Close-Up Photomicrograph of Well-Developed Burrow Structure: Conostichus, sp. Replaced With Siderite (Unit 35). No Observed Siderite was Present in Sandstone Surrounding Burrow.

Figure 54. Pocola Section: Close-Up Photomicrograph of Burrow Structure: Conostichus (?). Replaced With Siderite (Unit 35). Dark Material is of Siderite as Small Rhombs of Siderite along Laminae. Hammer Handle Shown along Left Margin for Scale.

Although considerable work could be done on the specific environments of biogenic sedimentary structures and trace fossils and on their relationship to apparent depositional energy conditions, it is clear that the major types present in the Hackett and Pocola Section suggest a very shallow marine to brackish environment. A detailed definition of environment based on the fauna identified is not possible at this time. However, the presence of Conostichus probably represents a near-shore marine environment and the other forms, excluding Chondrites, support a tidal flat to marginal bay or lagoonal environment. Based on its reported occurrence, Chondrites may range from shallow to deep water and from brackish to marine conditions.

Plant Fragments: Numerous fragments or impressions are recorded in both the Hackett and Pocola Sections. The preservation is such that only their gross characteristics can be described. They occur in the shales of the lower units in Hackett Section and in the major "fossil hash" zone in the Pocola Section (Zone VII, Unit 31). Figure 39 illustrates one such occurrence in the Pocola Section. Replacement by siderite or other material is not apparent.

Miscellaneous Forms: Figures 55 and 56 show what is tentatively identified as a *Scaphopoda*. Note the oblate structure in figure 56 which may be the stomach tube. Figures 57 and 58 are two unidentified microfossils from the Hackett Section.

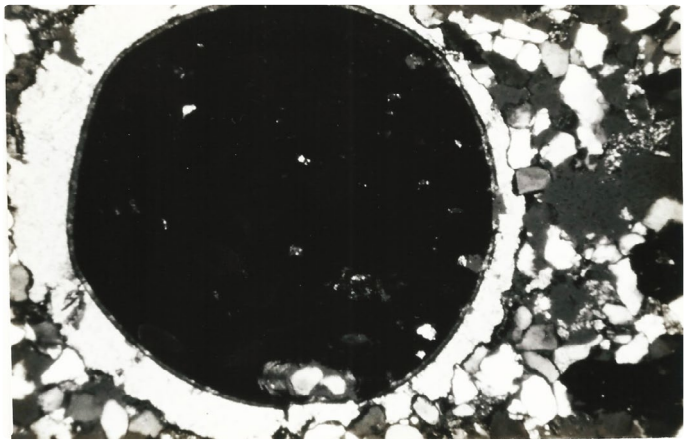

Figure 55. Hackett Section: Photomicrograph of Scaphopod (?). Interior of Tube Filled with Siderite (Dark), Calcite "Shell" Surrounding. Small Rhombs of Siderite in Interstices Among Quartz Gains. Sample DP-5, 10X, Crossed Nichols.

Figure 56. Hackett Section: Close-Up Photomicrograph of Scaphopoda (?). Showing "Stomach-Tube" Structure.), Calcite "Shell" Surrounding. A Few, Small Rhombs of Siderite Outside of "Shell" at Bottom. Sample DP-5, 40X, Crossed Nichols.

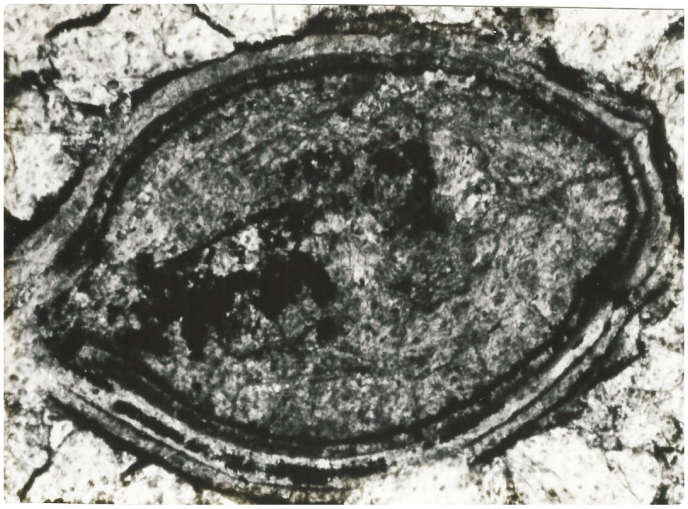

Figure 57. Hackett Section: Close-Up Photomicrograph of Unidentified Microfossil (Ostracod?). Sample H-17, 40X, Plane Light, From Siderite Zone II A Few,Small Rhombs of Siderite, 40X, Plane Light.

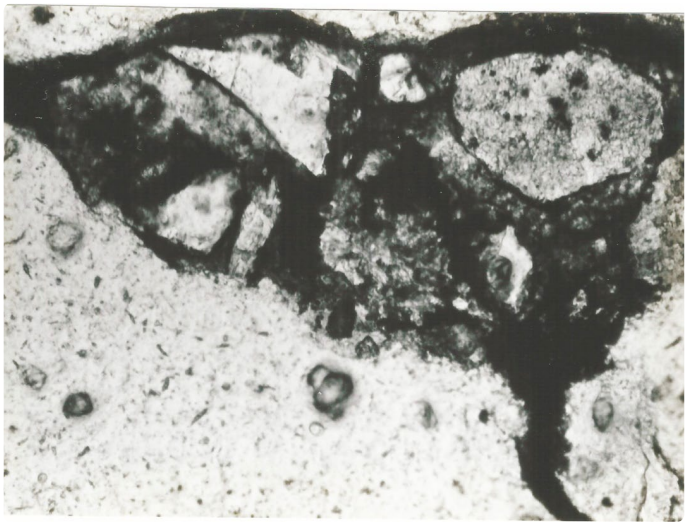

Figure 58. Hackett Section: Close-Up Photomicrograph of Unidentified Microfossil (Immature Gastropod?). Sample H-17, 40X, Plane Light, From Siderite Zone II A Few, Small Rhombs of Siderite Interior of Fossil Body.

Environments of Deposition

Lithological, textural and mineralogical characteristics of the siderite occurrences are summarized below with their possible paleoenvironmental and/or diagenetic implications. Evidence cited may be either complimentary or conflicting. These are:

A. Occurrence of cut-and-fill structures:
   1) Evidence for distributary channels, and/or
   2) Evidence for high-velocity bottom currents

B. Occurrence of multiple bedding types, e.g. thin, medium and thick, planar, and wavy, etc.:
   1) Evidence for widely fluctuating bottom currents, and/or
   2) Evidence for widely fluctuating sedimentation rate

C. Occurrence of subtle, rhythmic coarsening and fining upward sequences:
   1) Evidence for shallow water deposition, and/or
   2) Evidence for fluctuating depositional centers and/or sedimentation rate

D. Occurrence of mineralogically uniform sediment throughout Hackett and Pocola Sections:
   1) Evidence for similar source of sediment, and/or
   2) Evidence for relatively constant source of sediment over extended period of time

E. Occurrence of illite, with significant 2M polytype muscovite component, and kaolinite in nearly equal proportions:
   1) Evidence against exposure of sediments to marine conditions over extended period, and/or
   2) Evidence for abundant supply of large flakes of detrital muscovite (2M polytype) as a result of rapid erosion of igneous or metamorphic hinterland.

F. Occurrence of chert:
   1) Evidence for erosion of pre-existing consolidated rocks, and/or
   2) Evidence for relatively short transport and deposition of some sediment components.

G. Occurrence of bioturbation and burrows both associated and unassociated with siderite zones:
   1) Evidence that specific types of Arenicolities and other reported forms may be shallow water organisms with high tolerance to fluctuating salinity, and/or
   2) Evidence that burrowing organisms were indiscriminate with regard to feeding areas.

H. Lack of occurrence of Zoophycos and Nereites biogenetic structures:
   1) Evidence for shallow-water conditions, and/or
   2) Evidence that environment was unsuitable for such organism, irrespective of water-depth implications.

I. Lack of occurrence of thick and numerous channel deposits:
   1) Evidence for small tidal range, and/or
   2) Evidence for limited local source of elastic material.

J. Occurrence of coaly laminae in selected siderite zones:
   1) Evidence for proximity to coal beds (swamps), and/or
   2) Evidence for isolated islands containing coal swamps surrounded by marine conditions.

The following is a summary of the significant features of the siderite occurrences in the Hackett and Pocola Sections, with their paleoenvironmental and/or diagenetic implications:

K. Occurrence of siderite within current ripple marks and within flaser bedded and low-angle, cross-bedded intervals:
   1) Evidence for periodic influx of fine-grained sediment, influenced by abnormally high tide or by change in direction of local sediment source, and/or
   2} Evidence for favorable site of accumulation of fecal pellets, organic mud or primary sideritic material.

L. Presence of pock-marked bottoms and "slickensides" on flat top and throughout Type I siderite occurrences:
   1) Evidence for either gel-like or pelletal character of original mud, and/or
   2) Evidence for similarity to under clays: gel-like material would yield to produce slicken sides as a result of sediment loading.

M. Siderite occurrence with possible associated chamosite or pyrite:
   1) Evidence for a siderite precursor, and/or
   2) Evidence for a syndiagenetic product of fecal, organic-rich matter or primary siderite, and/or
   3) Evidence that pyrite is an epigenetic product after siderite.

N. Siderite occurrence associated with fossiliferous fragments as mud matrix and as partial to complete replacement of calcareous material:
   1) Evidence for syndiagenetic replacement of fossil material and/or
   2) Evidence for "siderization" of marine-dominated sediments.

O. Cryptocrystalline siderite in massive occurrences (Type I, II, II-A, III-A, IV and V) and crystalline siderite as tiny crystals along quartz grain boundaries in dispersed siderite occurrences (Type IV-A):
   1) Evidence for a syndiagenetic replacement of original calcareous (?) mud, unrelated to replacement of fossiliferous material by siderite, and/or
   2) Evidence for a two-stage syndiagenetic replacement.

P. Occurrence of burrows filled with siderite mud, and burrows filled with quartz grains of uniform size and minor siderite:
   1) Evidence for biologic redistribution of viscous organic material or of primary siderite occurring at depositional surface-water interface; if filled with sideritic mud, was derived from surface or mud with uniform composition; if filled with uniform-size quartz grains, was derived from surface of quartz grains without mud, and/or
   2) Evidence for scattered occurrence of original mud in topographically low areas, i.e. ripple-marked troughs, etc.

Q. Interruption of siderite bands by burrowing (Type III-A)
   1) Evidence for existence of original mud, primary siderite or sideritic precursor, and/or

2) Evidence of burrowing animals contemporaneous with deposition of original mud or primary siderite.

R. Siderite bands contain "gravity" bedding (Type III-A):
   1) Evidence for highly viscous character of original organic, calcareous (?) mud, and/or
   2) Evidence supporting the view that the top non-quartz layers were less viscous at water-mud interface due to effects of diluting currents, and/or
   3) Evidence for a two-stage syndiagenetic replacement,
   4) Evidence for flowage of viscous mud or addition of water from sands below, and/or
   5) Evidence that quartz grains were deposited as gel accumulated, sinking into viscous mass.

S. Trilobite fragment in siderite Type II:
   1) Evidence for lost stranger, and/or
   2) Evidence that parts of the exoskeleton was transported after molting, and/or
   3) Evidence for "siderization" of marine sediments.

T. Marine faunal zones as Type III:
   1) Evidence for storm debris brought into intertidal areas, and/or
   2) Evidence for marine influence.

U. Isolated fossi1 Conostrichus, replaced in total by siderite (with surrounding sediments clean) is not within 30 vertical feet of closest siderite zone:
   1) Evidence that syndiagenetic replacement of calcareous material was selectively pervasive, and/or
   2) Evidence of selective replacement of calcitic material via influence of local Eh-pH conditions within organic material of the remains of the organism, and/or
   3) Evidence of near-normal marine conditions in some Pocola stratigraphic units.

V. Siderite associated with coaly laminae (Type Ill, TI, III-A, and V):
   1) Evidence of proximity to plants and marsh or swamp, and/or
   2) Evidence for fluctuating character of depositional sequences in response to progradation or relative sea-level change, a minor transgression or regression cycle complex.

W. Siderite nodules reported in one thin unit only:
   1) Possible evidence for post-depositional marine influence, causing siderite to react to marine, high Ca^{+2} and SO_3^{-2} water via partial solution, and/or
   2) Shape may be a result of the instability in the presence of high Ca^{+2}, SO_3^{-2} in the subsurface produced by processes of associated organic zones.

X. Occurrence of siderite clasts in massive and cross-bedded sandstone:
   1) Evidence for distributary channels and/or
   2) Evidence for erosion and redeposition of primary or syngenetic siderite and/or
   3) Evidence for erosion and redeposition of organic-rich siderite precursor and/or
   4) Evidence for scattered occurrence of primary siderite or precursor.

Y. Siderite bands (IV-A) erosion, redistribution of very fine siderite material:
   1) Evidence for redistribution of pre-existing sediments containing sideritic material from up paleoslope, and/or
   2) Evidence for *in situ* syndiagenetic replacement of redistributed calcareous material.

Z. Occurrence of sideritic clay-size material within some black shale units:
   1) Evidence for erosion and redeposition of clay-size siderite from up dip into reducing environment of black shales, and/or
   2) Evidence for existence of organic matter syndiagenetically altering to siderite. Based on the above features and data presented previously, a shallow-water lagoonal, marginal bay, or tidal-flat environment is indicated by the bedded siderite occurrences and associated sediments, a view of which is supported by the lithologic data and interpretations previously presented. Some nearby sediments of probable marine origin (fossil-debris zones) could have been brought into the margins of a lagoon, tidal flats or isolated islands by storms or high rainfall and drainage not unlike the delta complex of the lower Mississippi River. Rapid deposition, followed by periods of slow deposition is clearly evident via the sedimentary structures. Some of the periods of slow deposition were of sufficient duration that clay-size material (a siderite precursor) or primary siderite was deposited in zones, remaining undisturbed until a new period of deposition again originated, shearing the upper surface of the zones and ripping-up some zones, depositing clasts down the slope via abnormally high-velocity currents of distributary channels. This was perhaps during the river's flood stage or during storm events.

Literature of the Period

Visher et al. [36] in work on the Pennsylvanian delta complexes in east central Oklahoma, indicate that the period was a major time of subsidence on the continental margin and a major period of onlap from the south to the north, The similarities in the delta patterns and basic depositional framework suggested to Visher et al. [36] that progradation was evident as a result of excess sediment supply in large deltaic complexes. Of special interest, however, is their observation that iron chlorite" (chamosite?), in addition to kaolinite and illite, suggest that the proportion of the clay minerals appeared to be related to the environment of deposition. For example, they indicate that the sandstone zones with the highest intensity of bioturbation generally have the highest illite and iron-chlorite content. They did not describe the chlorite mineral but it is apparently significantly more abundant than in the study area. Siderite in the form of rhombs less than 2 microns in size was reportedly associated with the iron chlorite.

Briggs, McBride and Moiola [37] suggest that the Pocola sediments "exhibit features indicative of deposition in a tidal flat environment." They also indicate that "middle to lower tidal flat deposits appear to comprise the bulk of the Pocola sequence, although shale dominated upper tidal flat deposits are also present."

Remarkable similarities exist between the upper Atoka Formation in the Pocola and Hackett area and the lower Devonian Uan Caza Formation in southern Tunisia [38], the upper Ordovician Bald Eagle Formation in the Central Appalachian miogeosynclinal sequence [39], and the Desmoinesian Bluejacket Sandstone in eastern Oklahoma [40]. All are interpreted as tidal flat-dominated sequences with similar occurrences of siderite (predominantly within shale intervals), thin fossil debris intervals (well-developed brackish fauna) and similar sedimentary structures and fining and coarsening upward sequence. Mud cracks, however, were reported in the above formations. They have not been recorded in the Hackett-Pocola Sections.

The preponderance of shallow water sedimentary structures [41], the rapidly fluctuating depositional rate, uniform clay-mineral content of kaolinite and illite, the minor fining and coarsening upward intervals, the mixed marine fauna intimately associated with coaly laminae taken all together indicate a marine-influenced marginal bay, lagoon and/or tidal flat environment, within or bordering a large deltaic complex with multi-cycle sediments possibly transported from the northeast [42].

The character of the sediments enclosing the bedded siderite zones (Types I, II, II-A and III-A) suggest that they may have been deposited in a shallow brackish or marine swamp environment, the siderite representing primary sediments. The sediments containing marine fauna and nodules (Types III and V), including *Conostichus* zones may have been deposited in an open shallow marine environment, with the associated siderite replacement being a syngenetic process generated by a readjustment to conditions within which primary siderite formation was dominant, or alternatively, being a syndiagenetic process, where the replacement was generated by Fe^{+2} -rich subsurface water. The environments of deposition, without a consideration of the implications of the siderite zones, can be defined with reasonable certainty. However, since a fauna that clearly supports the previously indicated environments has not been recovered, except for the thin marine fossil debris zones, and since the sedimentary structures could also be applicable to a marine environment of deposition, the environment of siderite genesis, therefore, assumes an important role in distinguishing between a marine and marginal marine or nonmarine environment.

Discussion of Siderite Genesis: Review of Literature

Siderite genesis has been studied extensively in various parts of the world and the physio-chemical requirements for siderite genesis are reasonably well documented [43-48]. Hem [49] explored the chemistry of iron and manganese is solution. Baas Becking, Kaplan and Moore [50] investigated the natural environment in terms of pH and oxidation-reduction potentials. The proposed depositional environment within which siderite occurs includes environments ranging from nonmarine, marginal marine to marine. James [27,51], 0'Rourke [52] and Lepp [53] summarize the prevailing views on the general subject of siderite occurrence. Many of the relevant reported occurrences are related to coal measures, occurring as nodules within dark shales.

Siderite stability

Berner [54] suggests that siderite is stable under severely restricted physio-chemical conditions. Thermodynamic data indicate that Eh and sulphide must be low, which is an unusual condition in marine sediments. Since a low Eh is the result of anaerobic bacterial decomposition of organic matter, and since dissolved sulfate is common in normal marine water, a reduction of sulfate to sulphide would occur and reversible redox equilibrium between sulfide in solution and H_2S in solution would develop, Berner [54] suggests that siderite is not stable with abundant sulfide. For siderite to be stable, sulfate reduction must be either nearly complete (i.e. achieving and diffusing H_2S or its formation is inhibited so that only the metastable sulfate exists. Pyrite, however, is stable under reducing conditions with abundant sulfide. Berner [55] in earlier work stated that for siderite to be stable relative to calcite, the concentration of Fe^{+2} must be greater than 5.0 percent that of calcium. Calcite will be dissolved and replaced by siderite if it is in contact with a solution containing ferrous ions in a concentration more than 0.66 percent that of calcium ions. In sea water, and marine sediments he reports that the ferrous iron is usually less than 0.10 percent that of calcium.

Non marine primary genesis

One view, therefore, suggests that primary siderite does not occur in open marine environments today but in swamps and other restricted basins where the ferric oxide hydrosols in river water attached to clay minerals could be separated and reduced to the ferrous state; but through removal of CO_2 by photosynthesis of nearby water plants, the bicarbonate formed would disassociate to cause the direct precipitation of siderite, associated with pyrite and some lignite deposits [56]. Ho and Coleman [57] support the view by describing siderite nodules (and associated diagenetic pyrite replacement) in the sediments below the swamps of the Atchafalaya Basin in the Mississippi Delta region. Oftedahl [58] also indicates a non marine origin for his sideritic ironstone. Rizzini [38] suggests a lagoonal depositional environment for the siderite formation. Wilson [59] reports the occurrence of siderite in underclays in South Wales as non marine.

Marine primary genesis

The extensive work on Pennsylvanian coal measures, however, appears to contradict the above view and indicates that freshwater, brackish and marine siderites occur. Williams [60] found siderite associated with three distinctive faunal groups, i.e. freshwater, restricted marine and marine. Williams

and Nickelsen [61] described a large siderite concretion containing marine fossils. Ferm [62] implied a marine and brackish offshore environment for the clay-ironstone nodules common in shales and dark-colored sandstones. Weber, Williams and Keith [63] found through C^{13}/C^{12} ratios a complete separation of freshwater siderite nodules from two marine siderite groups. Faunal associations strongly supported the freshwater and marine separation. They further indicate that freshwater siderite appears to contain more clay material than the marine variety and a threefold division is suggested by bulk chemistry [64].

Carbon and Oxygen isotopes

Hadi and Astin [65] applied carbon and oxygen isotopes to evaluate the diagenetic history on Upper Miocene sandstones containing abundant siderite. The marine siderites tend to be elliptical or lensoidal and internally fractured or fragmented, whereas the freshwater siderites are platy and internally homogeneous. Ferm and Williams [66] continued the threefold separation. Galimov and Mazur [67] also working with C^{13}/C^{12} ratios in siderite further support the separation into three environments of formation. Hallam [68] indicates a marine influence on the Liassic ironstones. Borchert [69] precludes a continental source of iron, drawing on the ocean as a veritable reservoir of iron in solution. Young [70] found ironstone concretions in the most seaward tip of a sandstone tongue as it grades into the marine Mancos Shale. Paull [71] reported clay-ironstone in the offshore faces of the Muddy Sandstone; Land [72] described siderite concretions in both the marine and marginal marine facies of the Fox Hills Sandstone. Cotter [73] describes siderite concretions in the Clawson Unit - an offshore shelf environment.

A syndiagenetic or epigenetic view partly reconciles the above conflict of reported occurrences with thermodynamic and solubility data. Fairbridge [56] suggests the rather common occurrence of a marine limestone metasomatically replaced by siderite. In such case, the $CaCO_3$ in the form of aragonite or high-magnesium calcite as porous oolites of calcarenites provides a host for later dolomitization and phosphatization. Just as certain pelecypods and brachiopods escape dolomitization, so also do they escape siderization, begin found with low Mg calcite intact in a matrix totally replaced by siderite (also see Bahrig [74]).

Chauvel and Dimroth [75] support a diagenetic origin for a siderite-rich zone deposited in a peritidal environment where calcareous muds were replaced by siderite. This alternate view would conserve the thermodynamic data and suggest a feasible alternate explanation for the occurrence of "marine" siderite containing marine fauna.

Syndiagenetic siderization could begin as most of the anaerobic bacteria have completed the sulfate-reduction in the presence of marine organic material, as fresh, reducing ferrous-charged subsurface water moves down dip from beneath a nearby ferrous-saturated lagoon, marsh, or tidal flats via permeable zones (sands of any thickness and clays, both still unconsolidated during this period) into calcareous marine sediments.

A Fe^{+2}-rich geochemical cell, reducing in character with older groundwater migrating down the hydraulic gradient may allow selective exchange of Ca^{+2} for Fe^{+2}. As the cell migrates down the hydraulic gradient and as siderization continues, the Fe^{+2}/Ca^{+2} ratio would decrease with an attendant decrease in bulk efficiency of the Fe^{+2} exchanges. Only densely crystalline calcite would escape total siderization.

C^{13}/C^{12} would be expected to be graduation from C^{13} depleted to C^{13} abundant, caused by a decreasing effect of the Fe^{+2} exchange and corresponding increase in Ca^{+2} over Fe^{+2} in solution below the sediment interface seaward. This trend is shown by Weber, Williams and Keith [63].

As Fe^{+2} replaces Ca^{+2}, C^{12} would be introduced in the siderite; but as the process decreases in the effectiveness of the Fe exchange, the C^{13} would begin to dominate. Although the C^{13}-enriched siderite is associated with a marine fauna, the siderite, as will be shown, is probably not syngenetic with the fauna but rather was probably formed in a brackish environment prevalent during part of the year; the fauna invaded the area as marine conditions returned. Alternately, if the siderite is syndiagenetic after replacement of calcareous material via a cell of siderization then the carbon isotope would indicate C^{13} enriched as indicated above.

Siderite replacement timing

Of particular significance to the timing of siderite replacement is the living echinoderm and its relatively porous skeletal structure. During early burial, however, calcite expels considerable magnesium which creates dense, low magnesium calcite plates showing optical continuity in thin-section. The period during which the calcite structure is most vulnerable to replacement by other cations of similar size is during the early porous stage just after burial.

As syndiagenesis proceeds the calcite crystal lattice may expel magnesium and take on iron, if present in sufficient quantity and if the ion is in a similar valence state. It is interesting to consider, however, that if the calcite is subjected to a slightly acidic environment, which weakens the calcium-carbonate bonds, and if ferrous and manganiferrous cations were present +2 in sufficient quantity (as Fe^{+2}exceeds 0.66 percent that of Ca), the calcium ion would be expelled from the calcite structure, leaving the magnesium but exchanging the calcium for the iron [76]. Further, if ferrous iron were in great supply, it would dominate the carbonate, forming siderite, with at least trace amounts of magnesium and other available metals.

Siderite usually consists of a solid solution series involving Fe^{+2}, Mn^{+2} and Mg^{+2} with carbonate. Table 12 shows the atomic and ionic radii. The atomic sizes shown indicate that the calcium ion and the ferrous ion are not of compatible atomic size and ·therefore could not share the carbonate anion to any great extent. Further, since the ionic radii shown for Ca and Fe cations (+2) are more similar in size than magnesium, any reordering or recrystallization would favor the ferrous iron not the magnesium [76].

Table 12

ATOMIC AND IONIC RADII OF Ca^{+2}, Mg^{+2}, Fe^{+2} and Fe^{+3}

	Atomic Radius	Ionic Radius
Calcium $^{+2}$	1.97Å	0.99Å
Magnesium $^{+2}$	1.60Å	0.65Å
Iron $^{+2}$	1.26Å	0.76Å
Iron $^{+3}$	1.26Å	0.64Å

Table 12. Atomic and Ionic Radii of Ca^{+2}, Mg^{+2}, Fe^{+2} and Fe^{+3}.

In addition, the ferric ion, because of its valance state, could not form a bond with the carbonate. An oxidizing environment would be required to break the ferrous carbonate bond in order to release the ferrous ion into solution for oxidation to the ferric state, forming various combination oxides. Based on the effect of organic complexes on mineral solubilities, considerable oxidizing energies would be required to alter a siderite that has such complexes within its ionic structure.

A late diagenetic replacement of calcite by siderite would therefore require: 1) a continuous acidic and reducing character of the pore fluids, and 2) a quantity of ferrous ions considerably greater than 0.66 percent relative to calcium ions in solution to adversely affect the dense recrystallized, reordered calcite crystal. Irregularities in the replacement fabric of calcite by siderite would be expected to be more common, which it is not. The echinoids alone suggest an early replacement of calcium carbonate mud or fossil fragments by siderite or its precursors. The echinoids are common in most of the siderite zones, suggesting that they occupied a tidal flat or related environment in addition to marine environment as suggested by their presence in the "fossil hash" zones.

Role of organic matter and bacteria

Organic matter and bacteria in sediments derived from bottom-dwelling animals and plant material play a significant role in mineral complexing, precipitation and reprecipitation. Akiyama [77], in a laboratory experiment, found that ferrous (and ferric) iron co-precipitated with dissolved organic matter. Under such conditions, ferrous iron, once precipitated, is prevented from going back into solution. This demonstrates that a siderite subjected to a marine condition would remain relatively stable. It may, however, be sufficiently unstable to change shape (nodules?). Further, Akiyama's work also indicates that the ferrous iron tended to precipitate with dissolved organic matter even in low concentration, below the solubility. Evans [78] reports that adenosine triphosphates (ATP) were unusually effective in altering the solubility characteristics of various cations and minerals common in sediments. Such complexing effects severely complicate pH-Eh relations of the siderite and pyrite stability fields [45].

They found that ATP, an organic acid and one of a wide variety of alanine and amino acids found in organic material to have a pronounced effect on relatively insoluble minerals, was mixed into solution with a number of common minerals, including siderite. The results indicate that siderite remained in solution at a pH of 7.5 while calcite was completely soluble between a pH range of 7.5 and 8.5. This supports the view that Fe must remain in solution while bacterial sulphide reduction goes to completion during a very early burial stage. Calcite was dissolved in the above experiment, leaving abundant CO_2 in various forms incorporated within organic compounds. This suggests the possibility that the sediments derived from certain animals that excrete bacteria containing ATP-type amino acids can alter aragonite but do not contain calcite during an early burial stage, because Ca^{+2} would be forced into solution as an organic complex and would not be capable of accepting an anion (CO_2 of HCO_3) with which to bond.

If calcium carbonate existed previously, before such an environment was established, it would tend to dissociate, possibly leaving a phospho-organic structure lasting throughout the early-burial reduction and highly bacterially active stage. The structure could serve as sites for future nucleation of siderite if Fe^{+2} persisted, or of calcite if Ca^{+2} dominated as in normal marine sediments. As organic materials were converted to other amino acid types via bacteria, recrystallization of calcite (and siderite if Fe^{+2} were present) could begin.

Significantly, bacterial alteration was likely relatively ineffective on large crystalline calcite masses within many bottom dwelling animals. The fine, originally calcareous material would be subject to attack, especially very small aragonitic and calcitic crystal structures. Some alteration of the larger calcite structures would be expected in the outer layers of the shell structure.

Bacteria, therefore, play a dominant role in the alteration of organic materials. Inorganic compounds of carbon, including carbonates, are produced, consumed, dissolved, precipitated, or changed in state by bacteria, the species of which is usually either anaerobic (reducing) or aerobic (oxidizing) in character [79]. Some forms can do both, depending on the conditions to which they are subjected, Iron-reducing bacteria are obviously very common in anaerobic conditions rich in iron. Their role in the formation of siderite is uncertain and difficult to assess but it may be a critical one on the basis of their probable vast population associated with the organic materials, especially organic or vegetal matter with high ferrous-iron content.

The presence of bacteria and the attendant production via their byproducts of amino acids would appear to inhibit primary siderite formation in sediments also undergoing sulphate reduction within organic or vegetal matter during earlier burial. A siderite-precursor, therefore, seems to be necessary. Perhaps it is a form of chamosite, or an organic complex not readily identified or pyrite. Evans [78] noted that when sodium silicate was dissolved in ATP, radiating microliths of an aluminum silicate was formed similar to chamosite.

Rohrlich, Price and Calvert [80] report in a description of recent chamosite, forming in a restricted marine basin of 0.025 parts per thousand salinity (effectively freshwater during parts of the year), that the material is spherical to ovoid fecal pellets consisting of submicroscopic crystal plates of chamosite arranged tangentially or radially around the

pellets (approximately 50-200 microns). We concluded from the above that fecal pellets from bottom dwelling (or burrowing?) animals can rapidly alter in part to chamosite. Subsequent syngenetic and syndiagenetic processes, however, depend upon bottom currents, depositional rate, animal activity and the previously mentioned limiting physio-chemical parameters [81,82].

If periodic currents were sufficiently strong to disaggregate organic or chamosite material, the finely divided suspension material would settle during periods of low velocity currents in areas distant from the source of organic matter, or chamositic material (iron-rich chlorite?). If the pellets were not subjected to strong currents, the pellets would merge into a highly viscous mass of organic matter of chamosite where in bacterial sulphate reduction could go to completion in the subsurface. Pyrite would be formed if sulphide reduction was not complete and was not diagenetically affected by oxidizing subsurface water, etc. The reduction would be limited only by the volume of reducible organic material present during very early burial. If ferrous ions were present, and if the other previously mentioned physio-chemical conditions were met, siderite would form by the alteration of chamosite and/or pyrite via the introduction of HCO_3 from an external source. Both Fe^{+2} and CO_2 would be already present, however. Silicate bonds of the chamosite would have to become unstable in such an environment, a problem reviewed by Cohen [83] without solution to date.

Oxidation of siderite

It is generally accepted that siderite forms as an early diagenetic mineral occurring in fluvial depositional systems, and it is unstable in oxidizing environments and destroyed in permeable sandstones that have experienced uplift and exposure to the atmosphere. The end-product, of course, is iron oxide, from mm-scale rhombs to concretions and complex bands of iron-oxide cement. The outcropping rocks of the Shinarump member of the Chinle Formation in Utah and Arizona have been examined in some detail [84].

Conclusions

In summary, for siderite to form syngenetically, the following criteria must be met.

Fe Input Requirement: Abnormally abundant Fe or Fe in solution or must in suspension be available in the surface water; possible under common conditions created by vast coal-forming swamps and under very special conditions such as involving iron-rich water of hot springs and volcanism dumped into river [27]. If iron of normally high concentration was transported in a river carrying a significant clastic load, the coarse elastics would be deposited upon reaching a bay, lagoon or tidal flat, but the iron as a colloid or in solution would be swept out to sea and deep water and deposited in the unoxidized form. During periods of limited or reduced elastic load the iron could settle relatively rapidly near the river's mouth

Ca+2 Abundance: Bottom conditions must be low in Ca^{+2}, probable in brackish water or marine-dominated swamps with abundant vegetal or organic matter; but sulphate reduction of organic matter must be buffered by high CO_2 or HCO_3, or other cation in great supply, or the sulphate reduction must have been completed previously.

Sulfate Reduction: Bottom conditions must either promote rapid sulphate reduction (possible where organic or vegetal material is present in only minor amounts or has previously been reduced through metastable FeS stage) or in a location where sulphate reduction is nil owing to the absence of specific organic material that is labile to sulphide reduction (only possible under special conditions where bacteria other than the sulphate-reducing type are present, e.g. iron-reducing bacteria, etc. form a consortium to assist in creating a reducing environment.

Low Eh: Bottom conditions must have low Eh, but pH could be alkaline; possible river supplies HCO3 and conditions are quiet (during periods of low deposition rate). Iron bacteria may produce low Eh.

Siderite Formation: Sulphate-reducing bacteria might not be present owing to Fe^{+2} in solution combining with available CO_2 or with HCO_3 to form $FeCO_3$, plus sulfide-degraded organic complexes

A primary origin for siderite is possible, if the above criteria are applicable. Organic material may only be scattered, creating local pyrite masses. The occurrence of so-called marine siderite, which is tacitly assumed to be primary in origin, can be reconciled with the above criteria only if it is assumed that syndiagenetic processes are also involved and are equally effective in forming siderite, especially in producing the "siderization" of calcareous and fossiliferous muds or fecal or other matter after burial. Siderite formation could begin as "primary" at the original depositional surface and cease after burial and syndiagenetic or epigenetic processes have gone to completion.

It is clear that if the above criteria for the formation of primary siderite cannot be reconciled in an open marine shelf-type environment, then a syndiagenetic process must be involved that incorporates the same criteria necessary for the formation of primary siderite, but post depositional in the sub-surface environment. Such an environment is readily adaptable to the criteria of siderite genesis. For a syndiagenetic origin of siderite in sediments deposited under marine conditions, the following environmental and physio-chemical criteria must be met:

Requirement:	Characteristics:
Fe Input:	Organic material with moderate amounts of Fe^{+2} or Fe^{+3} available on sea floor; possible as fecal or other organic-rich material and concentrated by bottom currents.

Deposition of Clastics:

Organic material is removed from normal marine physio-chemical conditions, probably as bacterial sulfate reduction begins, creating a reducing environment.

Sulphate Reduction and Ca^{+2} and Low Eh:

After burial, sulphate-reducing bacteria expel Ca^{+2} by diffusion [85] and produces pyrite during presence of sulphide until all the sulphate has been reduced and FeS2 has formed; any residual H2S (aq.) would be expelled by diffusion; possibly when Fe^{+2} and CO_2 or HCO_3 are transported from surrounding sediments containing other reduction processes, augmenting ions already undergoing nucleation as $FeCO_3$.

Replacement of calcite: "Siderization":

Fe^{+2}·dominates Ca^{+2} and replaces the calcite in porous areas within organisms and replaces calcareous mud; probable since during early burial, the structures of some organisms are susceptible to Fe^{+2} replacement of Ca^{+2} Excess Fe^{+2} and HCO_3 nucleate along quartz-grain boundaries to form small siderite euhedral structures.

Genesis of Siderite Types: A Paleoenvironmental Summary

The mechanisms involved in the origin of the bedded siderite types (I, II, II-A and III-A) are reasonably clear. They apparently cannot form syngenetically in a normal marine environment but could form under brackish conditions. This is supported by sedimentary structures, proximity to coal beds and thermodynamic data. The clasts contained in the proposed distributary channels were composed of sideritic material, although soft in character, prior to their erosion from bedded types. Burrowing of a gel-like primary siderite mud is evident, although the original mud may have been highly organic. The fossiliferous zones Type III), although marine in general character, were probably transported into a brackish environment capable of initiating syngeneic replacement of the calcareous material at the new depositional site or syndiagenetically after burial.

The siderite-replaced burrow structure (*Conostichus*) in the upper Pocola Section indicates a near-normal marine environment, if that form's paleoenvironmental significance is correct. That structure's replacement by siderite probably occurred syndiagenetically after the organism was buried by rapid deposition in a delta nearshore environment and marine water was displaced by an invading cell of Fe^{+2} enriched groundwater [26,86].

Dimroth [87] has explored the feasibility of some of the above mechanisms but did not accept the possibility of a syngenetic origin for siderite or a syndiagenetic siderite precursor (organic or calcareous mud) that permits siderization. He emphasized the importance of the oxidizing, turbulent environment above the sediment-water interface that prohibits siderite formation, but in periodically quiet conditions of low sediment influx, iron in suspension or as a colloid would settle and the ubiquitous iron-reducing bacteria could create reducing conditions. The reduced iron would readily combine with the abundant HCO_3 present in a lagoon or tidal flat environment to form syngenetic siderite.

Paleogeographic control of a siderite facies is a distinct possibility, within certain limits, if syndiagenesis plays the subordinate role in siderite genesis. For example, in the Pocola Section, marine conditions become dominant in Unit 35, below which a tidal flat or shallow bay environment prevailed with major distributary channels present in at least Units 31, 29, 27, 25 and 24 (See figure 9), the thin sandstone units in the lower sections being minor distributary channels running through a tidal flat environment. The bedded siderite may occupy an overbank position where channel abandonment isolated an area over a prolonged period of time allowing primary siderite to form in a quiet environment rich in Fe and HCO_3.

Intervals of the Hackett Section indicate a different relationship with marine conditions than in the Pocola Section. The fossiliferous zones probably represent storm deposits. Only one such zone occurs in the Pocola Section (Zone VIII). A tidal flat or bay environment persisted, however, in the remainder of the Hackett Section. Distributary channels are present in at least Units 6, 16, and 20 (See figure 4).

An expansion of C^{13}/C^{12} work on siderite may prove to be of value in further exploring the syndiagenetic replacement of calcareous and sideritic muds during deposition. A review of the major and minor element content of siderite, in view of the suggested thermodynamic behavior of siderite, could also clarify the timing of deposition and of consolidation of Type I siderite banding to establish either its syngenetic and/ orsyndiagenetic origin.

Research Update

An additional visit was made to the Hackett Section in 1990 for the purpose collecting additional samples to determine the carbonate content andfor preliminary evaluations of the remanent magnetism exhibited by Type I siderites (see figure 59).

Figure 59. Hackett Section: East Side of Road. Dr. Tom Alexander pointing to Base of Unit 5-Top of Unit 4 (see Figures 4, 5, and 6).Type I Sample (H-90): Siderite Zone III, Unit 8; at Right Ribbon. Principal Carbonates.

Principal Carbonates:

Duplicate samples were analyzed for carbonate and SiO_2 (see table 13). The samples are from a Type I Siderite Zone and consist of about 40% $FeCO_3$, 10% $MgCO_3$, 3% $CaCO_3$, and about 1.5% $MnCO_3$. The samples also contain 27% SiO_2, likely related to the presence of detrital quartz, which occurs within some types of siderite zones, e.g., Figures 30 and 43, the remaining 16% currently unknown. A full elemental scan would be of interest. And, a systematic unit by unit analysis would be required to assess the relation of the Fe, Mg, Ca, and $MnCO_3$ (and other elements) to the likely environment of deposition [88-91].

Analyzed For:	H-90A (wt.%)	(mol%)	CO_3 Rank (%)	H-90B (wt.%)	(mol%)	CO_3 Rank (wt.%)
$FeCO_3$	41.9	36.2	74.4	39.1	33.7	70.9
$MgCO_3$	9.4	11.2	16.7	11.5	13.6	20.9
$CaCO_3$	3.3	3.3	5.9	3.2	3.2	5.7
$MnCO_3$	1.7	1.5	3.0	1.4	1.5	2.5
SiO_2	25.9	43.1	-	29.1	48.4	-
Unknown	17.8			15.7		

Table 13. The samples are from a Type I Siderite Zone and consist of about 40% $FeCO_3$, 10% $MgCO_3$, 3% $CaCO_3$, and about 1.5% $MnCO_3$

In 1971, Sellwood [92] concluded, and confirmed here, that siderite was selectively precipitated near the sediment/water interfaces. The substrates were oxidizing in the upper sections containing ferric iron that precipitated as oxide and hydroxide, but when reduced ferrous iron at depth later allowed iron to combine with CO_2 forming siderite as the available organic matter decayed. Differing rates of sedimentation would produce rhythmic alternations of siderite bands and organic shales.

Mozley [93] and then Mozley and Carothers [94] developed and then applied an approach to distinguish early diagenetic siderites from marine and fresh-water depositional environments, which are characterized by distinctive compositional trends. They found that siderite from fresh-water environments are often relatively pure (i.e., greater than 90 mol% $FeCO_3$ and commonly attains end-member composition, whereas siderite from marine environments is always impure and has extensive substitution of Mg (up to 41 mol%) and to a lesser extent of Ca (up to 15 mol% for Fe in the siderite lattice. Also, marine siderite generally contains less Mn and has higher Mg/Ca ratio than fresh-water siderite. The subject samples in Table 13 place those results in neither category, marine or freshwater. Does this mean the results are indicating some intermediate environment? The SiO_2 present in the subject samples is considered the key in that it present in more than quartz grains but as a binding agent throughout the siderite lattace that locks the constituents within the lattice, making it resistant to weathering and oxidation relative to the siderites reported in the growing literature of siderite.

A few years later, Thyne and Gwinn [26] explored the sedimentology and stratigraphy of the Cretaceous Cardium Formation that are generally interpreted as indicating an offshore, shallow-marine shelf environment of deposition; however, geochemical and isotopic data suggested that pore water salinity varied widely during early diagenesis for much of the Cardium. In cases with little or no evidence of subaerial exposure of the sediments, Thyne and Gwinn [26] postulated that this apparent conflict can be resolved by allowing infiltration of early meteoric water (groundwater) into these subsurface nearshore sediments behind a mobile mixing geochemical zone. Infiltration of groundwater and movement of this geochemical cell interface was likely present during any phase of basin formation, whether transgressive or regressive marine environments. Evidence for the presence of this paleo aquifer is found in data from the early-diagenetic siderite cements of the Raven River Allomember and Carrot Creek Member of the Cardium Formation.

Dutton et al. [95], reported that, in a Wolfcampian age sandstone in the Val Verde Basin in southwest Texas, siderite rhombs occurring along quartz-grain boundaries were the earliest major cement to precipitate followed by siderite concentrating bands of up to 10 cm thick or in patchs, likely at the surface during periods of low sedimentation. They posit that the cement was formed in a methanogenic geochemical environment at a burial depth of about 400 feet from sea-derived pore fluids.

Then in 2015, Kim Y et al. [96], reported that iron hydroxide and iron oxyhydroxysulfate has been found in acid mine drainage (AMD) during anoxic bioreduction in the depositional environment of quiescent conditions under which Type I siderite forms in the presence of organic material. As sulphur concentration declined so would pyrite formation (iron sulfide (FeS)) and the remaining Fe^{+2} would tranport into the organic masses to form siderite ($FeCO_3$), and other carbonates if Mg, Ca, and/or Mn are available. Geochemical cells in the shallow aquifers just below the sediment-water interface are well known in environmental and in natural resource investigations. Further work is needed on these processes.

Natural remanent magnetism

Discussions involving the genesis of siderite should include considerations of its natural remanent magnetism and of the nature of its oxidation during thermal treatments [97]. Most work have been conducted on high-purity siderite samples, but the subject Type I siderites are not of high-purity FeS, but contain other metals as well as silicon (SiO_2) (see table 13). These would serve to fix any remanent magnetism at some time during consolidation of the Type I siderite band.

Type I siderite samples were subjected to a preliminary AF Demagnetization Treatment (i.e., over the range of 0 to 999 oersteds) by the junior author of this paper while at Texas A&M University. The results show that the samples exhibited high coercivity:

Initial State: AF 0: 6.45×10^{-5} emv, Std. Dev: 0.6 emv

Final State: AF 999: 5.94×10^{-5} emv, Std. Dev: 0.6 emv

Measured and Corrected Maximum Moment Intensity: 8.39×10^{-5}

The above indicates that Type I siderites, in occurring as dense bands, might be useful in establishing other constraints on the environmental conditions of the zone described in this paper (as suggested by Just et al. [98]).

General Conclusions

During the initial bacterial reduction of iron accompanying anaerobic bacterial methanogenesis, this increased the Fe^{+2} combined with the products of H_2S in solution during intermittent periods of low sedimentation. Each Type I interval represents quiescent periods with intervening high rates of sedimentation (from flooding, or faulting in sediment source areas). Later, well after deposition, pore fluids containing residual Fe^{+2} and pockets of organic materials (producing localized H_2S) precipitated the siderite within the interstices of the consolidating sediment.

The practical aspect of abundant early siderite is that formation inhibits later losses in porosity by compaction and quartz cementation as siderite-rich sandstones maintain higher porosity and permeability than siderite–poor sandstones. The best oil and gas reservoir quality in the Texas sandstones occurs in the siderite-cemented zones. Rossi et al. [88] confirm that siderite genesis and then dissolution generates significant secondary porosity and primary permeability in oil and gas reservoir sandstones, hence the interest in siderite over more than the past 20 years.

Acknowledgments

The writer thanked a number of people involved in the original investigation. Particular appreciation goes to Dr. Donald Baker (advisor), Department of Geology, Rice University, for his assistance in the development of the project and for his counsel throughout the investigation. Dr. James Lee Wilson was of particular assistance in the carbonate and faunal aspects of the project.

A number of students, adjuncts, and Professors were of assistance in the X-Ray diffraction analysis, and in the statistical treatment of the data. Dr. Ken Mc Millen, Mr. Kevin Biddle and Mr. Jon Van Wagoner (both Ph.D. candidates) of the Department of Geology made significant contributions at the time of the initial study during numerous discussions.

The writer also thanked the Chairman of Department of Geology and the Dean of Graduate Study of Rice University for awarding the senior author the Eleanor and Mills Bennett Fellowship, which supported the writer during a part of the initial research period. Funds and equipment used during the project were graciously supplied by the Department of Geology, Rice University, Dr. John J. W. Rogers, Chairman (1973-1975) and Dr. James Lee Wilson, Chairman, (1976). Dr. H. C. Clark conducted the preliminary work on the remnant magnetism on the samples. A note of thanks also went to Mr. Elze Henunen, Preparator, Department of Geology, for his assistance in thin-section preparation and in the design of the X-Ray diffraction mounts.

Special gratitude went to Mr. Norman F. Williams, State Geologist, Arkansas Geological Survey in Little Rock, Arkansas and his staff for their assistance during the field investigations. Associate Dr. Tom Alexander of Tulsa, Oklahoma was helpful at the field sites in obtaining additional samples for further studies on siderite. Finally, to Ms. Mary Margaret Wiley Campbell, a very special note of gratitude was expressed for her support in the field and in the home during the project and which continues today.

The authors declare no conflict of interest. Further, funding for the ongoing research was provided by the various employers of the senior author over the past four decades, none of which had a role in the design of the subject investigations; in the collection, analyses, or interpretation of data; or in the initial writing of this paper or in preparing the manuscript of this paper, or in the decision to publish the results herein. Funds were last made available for continuing the research on siderite by I2M Consulting, LLC in Houston and Seattle, which paid for recent laboratory costs. The authors have received no funds for covering the costs to publish the paper in Open Access. The authors also have no beneficial interests in the subject areas discussed herein. A special note of thanks is extended to Roger W. Lee, Ph.D. for his recent improvements in the manuscript.

References

1. Penrose RAF. The iron deposits of Arkansas, Little Rock. *Annual Report of the Geological Survey of Arkansas*. 1982; 1: 153.
2. Haley BR. Geology of Barker Quadrangle, Sebastian County and Vicinity, Arkansas. *Ark Geol Comm Inform Circ 20-C*. 1966; 76.
3. Haley BR, Hendricks TA. Geology of the Van Buren and Lavaca Quadrangles in parts of Clearfield and Center Counties. *Min Ind Expt Station Penn State Univ Bull*. 1971; 71: 37-51.
4. Houseknecht DW. Deltaic Facies of the Hartshorne Sandstone in the Arkoma Basin, Arkansas-Oklahoma Border. *Geol Soc Amer*. Centennial Field Guide – South Central Section. 1988; 91-92.
5. Haley BR, Hendricks TA. Geology of the Greenwood Quadrangle, Arkansas-Oklahoma. *Ark/geol Comm Infor Circ 20 F*. 1968.
6. Buchanan RS, Johnson FK. Bonanza Gas Field- A Model for Arkoma Basin Growth Faulting, in Geology of the Western Arkoma Basin and Ouachita Mountains, Oklahoma, Oklahoma City. *Geological Society*. 1968; 75-84.
7. Brigg G, Roeder D. Sedimentation and Plate Tectonics, Ouachita Mountains and Arkoma Basin, in Guidebook to the Sedimentology of Paleozoic Flysch and Associated Deposits, Ouachita Mountains, Arkoma basin, Oklahoma. 1975; 1-22.
8. Sutherland PK. Late Mississippian and Pennsylvanian depositional history in the Arkoma Basin area, Oklahoma and Arkansas. *Geological Society of America Bulletin*. 1988; 100(11): 1787-1802. doi: 10.1130/0016-7606(1988)100<1787:LMAPDH>2.3.CO;2
9. Koinm DN, Dickey PA. Growth faulting in McAlester basin of Oklahoma. *American Association of Petroleum Geologists Bulletin*. 1967; 51(5): 710-718.
10. Vedros SG, Visher GS. The Red Oak Sandstone: A hydrocarbon-producing submarine fan deposit. In: Stanley DJ, Kelling G (eds). Sedimentation in submarine canyons, fans and trenches. Stroudsburg, Pennsylvania, Dowden, Hutchinson and Ross, Inc., 1978; 292-308.
11. Houseknecht DW, Kacena JA. Tectonic and sedimentary evolution of the Arkoma foreland basin. In: Houseknecht DW (eds). Tectonic-sedimentary evolution of the Arkoma basin. Society of Economic Paleontologists and Mineralogists, Midcontinent Section, Guidebook, 1983; 1: 3-33.
12. Zachry DL. Sedimentary framework of the Atoka Formation, Arkoma basin, Arkansas. In: Houseknecht DW (eds) Tectonic-sedimentary evolution of the Arkoma basin. Society of Economic Paleontologists and Mineralogists, Midcontinent Section, Guidebook, 1983; 1: 34-52.
13. Grayson RC. Morrowan and Atokan (Pennsylvanian) conodonts from the northeast margin of the Arbuckle Mountains, southern Oklahoma. In: Sutherland PK, Manger WL (eds) The Atokan series and its boundaries: *Oklahoma Geological Survey Bulletin*. 1984; 136: 41-63.
14. Sutherland PK. Late Mississippian and Pennsylvanian depositional history in the Arkoma Basin area, Oklahoma and Arkansas. *Geological Society of America Bulletin*. 1988; 100: 1787-1802.
15. Zachry DL, Sutherland PK. Stratigraphy and depositional framework of the Atoka Formation (Pennsylvanian), Arkoma basin of Arkansas and Oklahoma. In: Sutherland PK, Manger WL (eds) The Atokan Series (Pennsylvanian) and its boundaries—A symposium. *Oklahoma Geological Survey Bulletin*. 1984; 136: 9-17.
16. Houseknecht DW. Evolution from passive margin to foreland basin: The Atoka Formation of the Arkoma basin, south-central U.S.A. In: Allen PA, Homewood P (eds). Foreland basins. *International Association of Sedimentologists Special Publication no. 8*, 1986; 327-345.

17. Suneson NH. Arkoma Basin Petroleum - Past, Present, and Future. Oklahoma Geological Survey, Originally published in Journal. Oklahoma City Geological Society. 2012; 63: 1.

18. Briggs G, McBride EF, Moiola RJ. Description of field trip stops. In: Guidebook to the Sedimentology of Paleozoic Flysch and Associated Deposits, Ouachita Mountains-Arkoma Basin, Oklahoma. 1975; 88-94.

19. Reinech HE, Wunderlich F. Classification and origin of flaser and lenticular bedding. *Sedimentology*. 1968; 11(1-2): 99-104.

20. Wunderlick F. Genesis and Environment of the Nellenkopfchenschichten in comparison with modern coastal environment of the German Bay. *J Sed Pet*. 1970; 40(1): 102-130. doi: 10.1306/74D71F00-2B21-11D7-8648000102C1865D

21. Folk RL, Ward WC. Brazos river bar: a study in the significance of grain size parameters. *J Sediment Petrol.* 1957; 27: 3-26,

22. Carroll D. Role of clay Minerals in the transportation of iron. *Geochimica et Cosmochimica Acta*. 1958; 14(1-2): 1-27.

23. Carroll D. Clay minerals: A guide to their x-ray identification. *Geol Soc Am Special Paper*. 1970; 126: 80.

24. Hower J, Mowatt TC. The mineralogy of illite and mixed layer illite/montmorillonites. *Am Mineralogist*. 1966; 51(5-6): 825-854.

25. Ludvigigson GA, Gonzalez LA, Metzger RA, et al. Meteoric Shhaerosiderite Lines and their Use for Papelohydrology and Paleoclimatology. *Geology*. 1998; 26(11): 1039-1042.

26. Thyne GD, Gwinn CJ. Evidence for a Paleoaquifer from Early Diagenetic Siderite of the Cardium Formation, Alberta, Canada. *J Sed Res*. 1994; 64(4): 726-732.

27. James HL. Chemistry of the iron-rich sedimentary rocks. *US Geol Surv*. 1966. doi: 10.3133/pp440W

28. Moore RC. Treatise on Invertebrate Paleontology. Part O, Arthropoda 1. *Geol Soc Am.* 1959; 0399-0402.

29. Chamberlain CK. Recent Lebensspuren in Nonmarine Aquatic Environments. In: The Study of Trace Fossils: A Synthesis of Principles, Problems, and Procedures in Ichnology. 1975; 431-458. doi: 10.1007/978-3-642-65923-2_19

30. Howard JD. Characteristic trace fossils in Cretaceous sandstones of the Book Cliffs and Wasatch Plateau, Central Utah Coals Bull. *Utah Geol Survey*. 1966; 80: 23-33.

31. Simpson S. On the trace-fossil Chondrites. *Quarterly Journal of the Geological Society*. 1956; 112: 475-499. doi: 10.1144/GSL.JGS.1956.112.01-04.23

32. Branson CC. New records of the Scyphomedusan Conostichus. *Okla Geol Notes.* 1961; 21 (5): 130-138.

33. Pfefferkorn HW. Note on Conostichus Broadheadi Lesquereau (trace fossil: Pennsylvania). *J Paleontology*. 1971; 45(5): 888-892.

34. Chamberlain CK. Bathymetry and paleoecology of Ouachita geosyncline of southeastern Oklahoma as determined by trace fossils. *AAPG Bull*. 1971; 55(1): 34-50.

35. Fager EW. A sand-bottom epifaunal community of invertebrates in shallow water. *Limnol And Oceanog*. 1968; 13(3): 448-464. doi: 10.4319/lo.1968.13.3.0448

36. Visher GS, Saitta D, Phillips RS. Pennsylvanian delta patterns and petroleum occurrences in eastern Oklahoma: *Am Assoc Petroleum Geologists Bull*. 1971; 55(8): 1206-1230.

37. Briggs G, McBride EF, Moiola RJ. Description of field trip stops. In: Guidebook to the Sedimentology of Paleozoic Flysch and Associated Deposits, Ouachita Mountains-Arkoma Basin, Okla. 1975; 88-94.

38. Rizzini A. Sedimentary sequences of Lower Devonian sediments Uan Caza Formation, South Tunisia. A Casebook of Recent Examples and Fossil Counterpart, Springer-Verlag. New York. 1975; 187-195.

39. Thompson AM. Clastic coastal environments in Ordovician Molasse, Central Appalachians. In: Ginsburg RN (eds). Tidal Deposits: A Casebook of Recent Examples and Fossil Counterparts. Springer-Verlag, New York. 1975; 135-143. doi: 10.1007/978-3-642-88494-8_16

40. Visher GS. A Pennsylvanian interdistributary tidal-flat deposit. A Casebook of Recent Examples and Fossil Counterparts. Springer-Verlag, New York. 1975; 179-185. doi: 10.1007/978-3-642-88494-8_21

41. Reinech HE, Wunderlich F. Classification and origin of flaser and lenticular bedding. *Sedimentology*. 1968; 11 (1-2): 99-104.

42. Bucke DP. Effect of Diagenesis upon Clay Mineral Content of interlaminated Desmoinesian Sandstones and Shales in Oklahoma. Ph.D. Dissertation, University of Oklahoma, Norman. 1969; 130.

43. Krumbein WC, Garrels RM. Origin and classification of chemical sedimentsin terms of pH and oxidation-reduction potentials. *J Geol.* 1952; 60(1): 1-33.

44. Huber NK. The environmental control of sedimentary iron minerals. *Economic Geol*. 1958; 53(2): 123-140. doi: 10.2113/gsecongeo.53.2.123

45. Garrels RM, Christ CL. Solutions, Minerals and Equilibrium. Harper and Row. NY, 1965; 222.

46. Curtis CD, Spears DA. The formation of sedimentary iron minerals. *Economic Geol*. 1968; 63(3): 257-270. doi: 10.2113/gsecongeo.63.3.257

47. Garrel RM, MacKenzie FT. Evolution of Sedimentary Rocks. W. W. Horton Co., NY. 1971; 379.

48. Wolf KH, Chilingariar GV. Digenesis, IV, Developments in Sedimentation. Elsevier, Amsterdam-London-New York-Tokyo. 51: 1994529.

49. Hem JD. Chemical factors that influence the availability of iron and manganese in aqueous systems. *Geol Soc America Bull.* 1972; 83: 443-450.

50. Bass-Becking LGM, Kaplan IR, Moore D. Limits of the natural environment in terms of pH and oxidation-reduction potentials. *J Geol.* 1960; 67(3): 243-283.

51. James HL. Sedimentary facies of iron formation. *Economic Geol*. 1954; 49: 235-293.

52. 0'Rourke JE. Paleozoic banded iron-formations. *Economic Geol*. 1961; 56(2): 331-361. doi: 10.2113/gsecongeo.56.2.331

53. Lepp H. Geochemistry of Iron: Benchmark Papers in Geology. *Halsted Press*. 1975; 18: 320.

54. Berner. Principles of chemical Sedimentology. McGraw-Hill, NY. 1971; 240.

55. Berner RA. Sedimentary pyrite formation. *Am J Sci*. 1970; 268 (1): 1-23. doi: 10.2475/ajs.268.1.1

56. Fairbridge RW. Develpoments in Sedimentology. *Diagenesis in Sediments*. Amsterdam, Elsevier Press, Chapter 2, 1967; 19-89. doi: 10.1016/S0070-4571(08)70841-0

57. Ho C, Coleman JM. Consolidation and cementation of recent sediments in the Atchafalaya Basin. *Bull Geol Soc America.* 1969; 80: 183-192.

58. Oftedahl C. A sideritic ironstone of Jurassic Age. In: Beitstad-fjorden, Tréndelag: Norsk Geologisk Tidss krift. 1972; 52: 123-134.

59. Wilson MJ. The origin and geological significance of the South Wales Underclays. *J Sed Pet*. 1965; 35(1): 91-99. doi: 10.1306/74D711F9-2B21-11D7-8648000102C1865D

60. Williams EG. Marine and Fresh Water Fossiliferous Beds in the Pottsville and Allegheny Groups of Western Pennsylvania. *Journal of Paleontology*. 1958; 34(5): 908-922.

61. Williams EG, Nickelsen RP. Correlation of the Pottsville and Lower Allegheny Series in parts of Clearfield and Center Counties. *Min Ind Expt Station Penn State University Bull.* 1958; 71: 37-50.

62. Ferm JD. Petrology of some Pennsylvanian sedimentary rocks. *Journal of Sedimentary Petrology*. 1962; 32(1): 104-123. doi: 10.1306/74D70C54-2B21-11D7-8648000102C1865D

63. Weber JN, Williams EG, Keith ML. Paleoenvironmental significance of carbon isotopic composition of siderite nodules in some shales of Pennsylvanian age. *Journal of Sedimentary Petrology*. 1964; 34(4): 814-818.

64. Weber JN, Williams EG. Chemical composition of Siderite Nodules in the environmental classification of shales. *AAPG Bull.* 1965; 49(3): 362.

65. Hadi ARA, Astin TR. Genesis of Siderite in the Upper Miocene Offshore Sarawak: Constraints on Pore Fluid Chemistry and Digenetic History. AAPG International Conf. & Exhibition, Kuala Lumpur, Malaysia. *Geol Soc Malaysia Bull.* 1994; 37: 395-413.

66. Ferm JD, Williams EG. Characteristics of a carboniferous marineinvasion in western Pennsylvania. *J Sed Res*. 1965; 35(2): 319-330. doi: 10.1306/74D71262-2B21-11D7-8648000102C1865D

67. Galimov EM, Mazur VM. Living conditions of fauna and facies of sedimentation, in relation to isotopic composition of carbon in siderites: Geologiya i Razvedka, no. 10, 26-32, in Trans. *International Geology Rev*. 1972; 15(9): 1075-1080. doi: doi.org/10.1080/00206817309475987

68. Hallam A. Depositional environment of British Liassic ironstones considered in the context of their facies relationships. *Nature*. 1966; 209: 1306-1309. doi: 10.1038/2091306a0

69. Borchert H. Genesis of marine sedimentary iron ore. *Trans Inst Mining Metallurgy*. London. 1960; 69: 261-279.

70. Young RG. Sedimentary facies and intertunging in the Upper Cretaceous of the Book Cliffs, Utah-Colorado. *Geol Soc America Bull*. 1955; 66(2): 177-202.

71. Paull RA. Depositional history of the Muddy Sandstone, Big Horn Basin, Wyoming. *Wyoming Geol Assoc 17th Ann Field Conf Guidebook*. 1962; 102-117.

72. Land CB. Stratigraphy of Fox Hills Sandstone and associated formations, Rock Springs Uplift and Wamsutter Arch area. *Sweetwater County, Wyoming Colo Sch Mines Quart*. 1972; 67(2): 69.

73. Cotter E. Late Cretaceous sedimentation in a low-energy coastal zone: the Ferron Sandstone of Utah. *J Sed Pet*. 1975; 45(3): 669-685. doi: 10.1306/212F6E0B-2B24-11D7-8648000102C1865D

74. Bahrig B. The Formation of Alternating Chalk / Siderite Units During the Neogene in the Black Sea – An Example of Climatic Control of Early Diagenetic Processes. Chapter 6, Diagenesis IV. 1994; 133-153.

75. Chauvel JJ, Dimroth E. Facies types and depositional environment of Sokoman Iron Formation, Central Labrador Trough, Quebec, Canada. *J Sed Pet*. 1974; 44(2): 299-327. doi: 10.1306/74D72A1D-2B21-11D7-8648000102C1865D

76. Rodrigues AG, De Ros LF, Neumann R, Borghi L. Paleoenvironmental Implications of Early Diagenetic Siderites of the Paraiba do Sul Deltaic Complex, Eastern Brazil. *Sedimentary Geology*. 2015; 323: 15-30. doi: 10.1016/j.sedgeo.2015.04.005

77. Akiyama T. Interactions of ferric and ferrous irons and organic matter in water environment. *Geochemical J*. 1973; 7(3): 167-177. doi: 10.2343/geochemj.7.167

78. Evans WD. The organic solubilization of minerals in sediments. In: Advances in Organic Geochem. 1960; 263-270.

79. ZoBell CE. Geochemical Aspects of the Microbial Modification of Carbon Compounds. In: Advances in Organic Geochemistry. 339-356.

80. Rohrlich V, Price NB, Calvert SE. Chamosite in the recent sediments of Loch Stive, Scotland. *J Sed Pet*. 1969; 39(2): 624-631. doi: 10.1306/74D71CE9-2B21-11D7-8648000102C1865D

81. Talbot MR. Ironstones in the Upper Oxfordian of Southern England. *Sedimentology*. 1974; 21(3): 433-450. doi: 10.1111/j.1365-3091.1974.tb02069.x

82. Schoen R. Clay minerals of the Silurian Clinton Ironstones, New York State. *J Sed Pet*. 1964; 34(4): 855-863.

83. Cohen E. The nature of silicates and carbonates of iron on the Northampton Sand Iron stone of central England. In: Symposium sur les Gisements de Fer du Monde, XIX Congress Géologique International, Alger, Chapter XIII. 1952; 466-471.

84. Burgess DT, Kettler RM, Loope DB. The Geologic Contect of Wonderstone: A Complex, Outcrop-Scaled Pattern of Iron-Oxide Cement. *J Sed Res*. 2016; 86(5): 498-511. doi: 10.2110/jsr.2016.35

85. Presley BJ, Kaplan IR. Changes in dissolved sulfate, calcium and carbonate from interstitial water of near-shore sediments. *Geochemica et Cosmochimica Acta*. 1968; 32(10): 1037-1043. doi: 10.1016/0016-7037(68)90106-3

86. Machemer SD, Hutcheson I. Geochemistry of Early Carbonate Cements in Cardium Formation, Central Alberta. *J Sed Pet*. 1988; 58(1): 136-147. doi: 10.1306/212F8D37-2B24-11D7-8648000102C1865D

87. Dimroth E. Paleoenvironment of iron-rich sedimentary rocks. *Geologische Rundschau*. 1975; 64(1): 751-767. doi: 10.1007/BF01820694

88. Rossi C, Marfil R, Ramseyer K, Permanyer A. Facies-Related Diagenesis and Multiphase Siderite Cementation and Dissolution in the Reservoir Sandstones of the Khatatba Formation, Egypt's Western Desert. *J Sed Pet*. 2001; 71(3): 459-472. doi: 10.1306/2DC40955-0E47-11D7-8643000102C1865D

89. Khim BK, Choi KS, Park YA, Oh JK. Occurrence of Authigenic Siderites in the Early Holocene Coastal De[posit in the West Coast of Korea: An Indicator of Depositional Environment. *Geosciences Journal*. 1999; 3(3): 163-170. doi: 10.1007/BF02910272

90. Macaulay CI, Haszeldine RS, Fallick AE. Distribution, Chemistry, Isotopic Composition and origin of Diagenetic Carbonates: Magnus Sandstone, North Sea. *J Sed Pet*. 1993; 63(1): 33-43. doi: 10.1306/D4267A82-2B26-11D7-8648000102C1865D

91. Hart BS, Longstaffe FJ, Plint AG. Evidence for Relative Sea Level Change from Isotopic and Elemental Composition of Siderite in Cardium Formation, Rocky Mountain Foothills. *Bull Canadian Petrol Geol*. 1992; 40(1): 52-59.

92. Sellwood BW. The Genesis of Some Sideritic Beds in the Yorkshire Lias (England). *Journal of Sedimentary Petrology*. 1971; 41(3): 854-858. doi: 10.1306/74D7237E-2B21-11D7-8648000102C1865D

93. Mozley PS. Relation Between Depositional Environment and the Elemental Composition of Early Diagenetic Siderite. *Geology*. 1989; 17(8): 704-706. doi: 10.1130/0091-7613(1989)017<0704:RBDEAT>2.3.CO;2

94. Mozley PS, Carothers WW. Element and Isotopic Composition of Siderite in the Kuparuk Formation, Alaska: Effect of Microbial Activity and Water/Sediment Interaction on Early Pore-Water Chemistry. *J Sed Petrol*. 1992; 62(4): 681-692. doi: 10.1306/D4267988-2B26-11D7-8648000102C1865D

95. Dutton SP, Hamlin HS, Folk RL, Clift SJ. Early Siderite Cementation as a Control on Reservoir Quality in Submarine Fan Sandstones, Sonora Canyon Gas Play, Val Verde Basin, Texas. In: Siliciclastic Diagenesis and Fluid Flow: Concepts and Applications, SEPM Special Publication No. 55. *Soc Sed Geol (SEPM)*. 1996; 223-250.

96. Kim Y, Lee Y, Roh Y. Microbial Synthesis of Iron Sulfide (FeS) and Iron Carbonate ($FeCO_3$) Naoparicles. *J Nanosci Nanotechnol*. 2015; 15(8): 5794-5797.

97. Pan Y, Zhu R, Banerjee SK, Gill J, Williams Q. Rock Magnetic Properties Related to Thermal Treatment of Siderite: Behavior and Interpretation. *J Geo Phy Res*. 2000; 105(B1): 783-794. doi: 10.1029/1999JB900358

98. Just J, Nowaczyk NR, Sagnotti L, et al. Environmental control on the occurrence of high-coercivity magnetic minerals and formation of iron sulfides in a 640 ka sediment sequence from Lake Ohrid (Balkans). *Biogeosciences*. 2016; 13(7): 2093-2109. doi: 10.5194/bg-13-2093-2016

99. Ballard WW. Subsurface Study of Morrow and Atoka Series in Part of Arkansas Valley of Western Arkansas. *AAPG Bull*. 1957; 41(2): 263-277.

Appendices

Appendix A: Cumulative-Arithmetic Curves

Hackett Section

- Grain-Size Data
- Cumulative Curves

Pocola Section

- Grain-Size Data
- Cumulative Curves

Standard Deviation Calculations

Appendix B: Thin-Section Descriptions

- Hackett Section Samples
- Pocola Section Samples